Toxicology in Vitro 86 (2023) 105510

Contents lists available at ScienceDirect

Toxicology in Vitro

journal homepage: www.elsevier.com/locate/toxinvit

Multiple endpoint *in vitro* toxicity assessment of a prototype heated tobacco product indicates substantially reduced effects compared to those of combustible cigarette

Fiona Chapman [a,*], Edgar Trelles Sticken [b], Roman Wieczorek [b], Sarah Jean Pour [b], Ole Dethloff [b], Jessica Budde [b], Kathryn Rudd [a], Elizabeth Mason [a], Lukasz Czekala [a], Fan Yu [a], Liam Simms [a], Thomas Nahde [b], Grant O'Connell [a], Matthew Stevenson [a]

[a] *Imperial Brands PLC, 121 Winterstoke Road, Bristol BS3 2LL, UK*
[b] *Reemtsma Cigarettenfabriken GmbH, an Imperial Brands PLC Company, Albert-Einstein-Ring-7, D-22761 Hamburg, Germany*

ARTICLE INFO

Editor: Dr. P Jennings

Keywords:
Heated tobacco
Cigarette
Aerosol chemistry
Genotoxicity
Mutagenicity
High content screening

ABSTRACT

This study aimed to compare the aerosol chemistry and *in vitro* toxicological profiles of two prototype Heated Tobacco Product (p-HTP) variants to the 1R6F Reference Cigarette. In the neutral red uptake screen the p-HTPs were 37–39-fold less potent than 1R6F, in the micronucleus assay, responses to the p-HTPs were 8–22-fold less, and in the Ames test mutagenicity was weak or removed compared to 1R6F. The cardiovascular scratch wound assay revealed 58-fold greater wound healing impairment following exposure to 1R6F smoke extracts than the p-HTPs. Furthermore, in seven cell stress-related high content screening endpoints (cell count, cytochrome *c* release, mitochondrial membrane potential, GSH depletion, NFkB translocation, phosphorylation of c-jun and phosphorylation of H2AX), at 4 and 24 h, responses were substantially greater to 1R6F smoke extracts at comparable nicotine levels. The reduced *in vitro* effects of the p-HTPs were attributed to substantial reductions (90–97%) in selected HPHCs measured compared to in 1R6F smoke. The multiple endpoint *in vitro* assessment approach provides greater mechanistic insight and the first reported toxicological characterisation of these p-HTPs in the literature. Overall, the findings contribute to the growing weight of evidence that HTPs may offer a reduced harm mode of nicotine delivery to adult smokers.

1. Introduction

Combustible tobacco smoking is recognised worldwide as a major causative factor of serious diseases in smokers, including lung cancer, heart disease and emphysema (International Agency for Research on Cancer, 2012; United States Surgeon General, 2010; US Department of Health and Human Services, 2014). There is increasing evidence that next generation products (NGPs), for example, e-cigarettes, may provide an alternative mode of nicotine delivery for adult smokers, but with less smoking-related disease risk due to exposure to fewer and lower levels of harmful chemicals than with cigarette smoke (McNeill et al., 2018; Royal College of Physicians, 2016). The availability of such NGPs to adult smokers supports the public health concept of tobacco harm reduction (THR), where adult smokers who do not or choose not to quit have the option to transition to potentially reduced risk nicotine products (O'Leary and Polosa, 2020). It is proposed that nicotine products sit on a risk continuum, where combustible cigarettes pose the highest risk to adult smokers, and medically licensed nicotine replacement therapies

Abbreviations: ALI, Air-liquid interface; bPBS, (Smoke/ aerosol) bubbled phosphate buffered saline; ECMN3, Concentration required to reach three-fold micronucleus induction above background levels; GSH, Glutathione; GSSG, Glutathione disulphide; HCI, Health Canada Intense (smoking regime); HCS, High content screening; HPHCs, Harmful and potentially harmful constituents; HTP, Heated tobacco product; LOGEL, Lowest observed genotoxic effect level; MMP, Mitochondrial membrane potential; MN, Micronucleus/ micronuclei; NGP, Next generation product; NNK, N-nitrosonornicotine; NNK, Nicotine-derived nitrosamine ketone; NRU, Neutral red uptake (assay); p-HTP, Prototype heated tobacco product; PAH, Polycyclic aromatic hydrocarbon; RPD, Relative population doubling; RWD, Relative wound density; RWD50, Time taken for the initial wound to close to 50% of its original area; SAEIVS, Smoke aerosol exposure *in vitro* system; THR, Tobacco harm reduction; TPM, Total particulate matter; TSNAs, Tobacco specific nitrosamines.

* Corresponding author.
E-mail address: Fiona.Chapman@uk.imptob.com (F. Chapman).

https://doi.org/10.1016/j.tiv.2022.105510
Received 28 September 2021; Received in revised form 22 October 2022; Accepted 31 October 2022
Available online 11 November 2022

the least, with NGPs between these, and towards the lower risk end of the scale (McNeill and Munafò, 2013; Zeller, 2019).

Heated tobacco products (HTPs) form a growing NGP category; the majority of these products' designs are based around a battery powered device containing an element which heats a consumable tobacco insert (stick) to produce an aerosol inhalable by the adult smoker (Smith et al., 2016; Eaton et al., 2018). This aerosol, the product of heating the tobacco as opposed to burning, as is the case with combustible cigarette smoking, has been evidenced to contain substantially fewer and lower levels of harmful and potentially harmful compounds (HPHCs) than found in cigarette smoke (Mallock et al., 2018; Perezhogina et al., 2021; Schaller et al., 2016; Jaccard et al., 2017; Eaton et al., 2018; Forster et al., 2018; Bentley et al., 2020). The reduced levels of such chemicals in HTP aerosols has been demonstrated to translate directly to reduced levels of biomarkers of exposure measured in adult smokers upon transition to exclusive HTP use in controlled clinical settings, and further to this, nicotine delivery and consumer satisfaction (through urge to smoke measures) remain comparable between combustible cigarette smoking and HTP use (Picavet et al., 2016; Brossard et al., 2017; Sakaguchi et al., 2014; Ogden et al., 2015; Roulet et al., 2019; Akiyama and Sherwood, 2021). This evidence supports the HTP category's potential as a tool in THR, by providing adult smokers with an alternative means of nicotine delivery but with reduced or removed exposure to disease-related HPHCs, coupled with adult smoker satisfaction and acceptance.

Furthermore, the chemical differences between HTP aerosols and cigarette smoke can be correlated with reductions in *in vitro* toxicological effects (Hattori et al., 2020; Schaller et al., 2016; Dusautoir et al., 2021; Breheny et al., 2017; Jaunky et al., 2018; Kogel et al., 2015; Taylor et al., 2018; Wang et al., 2021; Scharf et al., 2021; Horinouchi and Miwa, 2021). A number of studies have demonstrated, in gold standard *in vitro* regulatory toxicity tests like the micronucleus (MN), Ames bacterial reverse mutation, and neutral red uptake (NRU) (cytotoxicity) assays, reduced, or even removed, effects upon exposure with HTP aerosol samples compared to cigarette smoke samples (Jaunky et al., 2018; Murphy et al., 2018; Godec et al., 2019; Thorne et al., 2020; Crooks et al., 2018; Leigh et al., 2018). In addition, these reduced effects have been observed in cardiovascular disease-related *in vitro* assessments (Poussin et al., 2016; van der Toorn et al., 2015), in multiple endpoint and systems biological assessments and even at the transcriptomic level (Poussin et al., 2018; Kogel et al., 2015; Iskandar et al., 2018; Gonzalez-Suarez et al., 2016).

Several studies have applied high content screening (HCS) approaches, encompassing a number of cellular stress-related endpoints, to compare HTP products against cigarette comparator samples, and have observed markedly reduced, or even absent, effects of the HTP samples (Kogel et al., 2015; Taylor et al., 2018). A HCS approach can provide high throughput, multiple endpoint mechanistic indications of cell stress, which may lead to cell death, or alternatively lead to cellular dysfunction, with high sensitivity, and has been widely utilised in the assessment of NGPs (Kogel et al., 2015; Czekala et al., 2019; Gonzalez-Suarez et al., 2016). Here, as part of our wider analyses, we investigated the effects of two prototype HTP variants (p-HTPs) and the 1R6F Reference Cigarette, on seven HCS endpoints associated with cell stress. The first measure (i) was of cell count, to indicate overall cytotoxicity within the treated cell populations. Release of cytochrome *c* (ii) from the mitochondria is an early stage of mitochondria-driven apoptosis (Nur-E-Kamal et al., 2004); mitochondrial stress, for example, through changes in functioning of the respiratory chain, or release of cytochrome *c* and other pro-apoptotic proteins, can be indicated by changes in mitochondrial membrane potential (MMP) (iii) (Hüttemann et al., 2011). Reductions of glutathione (GSH) levels (iv) through its oxidation to glutathione disulphide (GSSG) can indicate the action of this cellular defence mechanism in response to the presence of reactive oxidative species (Czekala et al., 2019; Gonzalez-Suarez et al., 2016). Further to this, decreases in GSH levels following exposure to cigarette smoke samples have been attributed to formation of irreversible conjugates with smoke constituents such as carbonyls (van der Toorn et al., 2015). Transcription factor, NfκB, is a fast responder to cellular stress, including the presence of toxins, oxidative stressors and pro-inflammatory mediators and is instrumental in the inflammatory response, in addition to its roles in apoptosis and cell proliferation, among other cellular processes (Trask Jr., 2012; Liu et al., 2017); its translocation to the nucleus following exposure was measured here to assess the presence of such cell stress-related responses (v). Phosphorylation of AP-1 transcription factor component, c-jun, is a process involved in regulation of cellular stress responses such as cell cycling and apoptosis (Dreij et al., 2010) and was used here to indicate such (vi). Phosphorylation of H2AX (γH2AX) at the site of DNA double strand breaks was used as an indicator of overall induced DNA damage (vii) (Garcia-Canton et al., 2014; Motoyama et al., 2018).

Combination of multiple endpoints in toxicological assessments can provide a greater weight of evidence to the potential mechanistic effects, and can even provide information on relative potency, of different test articles (Chapman et al., 2020; Wilde et al., 2018). Therefore, we also extended our *in vitro* assessment to additional regulatory toxicological endpoints, the MN, NRU, and Ames tests. Cigarette smoking is also reportedly associated with endothelial damage and impaired repair (wound healing) of this, and leads to the inflammatory processes precursory to atherosclerosis (Fearon et al., 2012; Fearon et al., 2013). The cardiovascular scratch wound assay has been demonstrated as an indicator of wound healing potential upon chemical exposure (Bishop et al., 2020), therefore this assay was also utilised here.

In light of the evidence in the scientific literature that HTP aerosols generally contain substantially fewer and lower levels of chemicals, including HPHCs, and this can be linked to decreased toxicological responses (Schaller et al., 2016; Dusautoir et al., 2021; Jaunky et al., 2018), this study aimed to compare the chemical composition of, and *in vitro* biological responses to, two p-HTP variants' aerosols against those of the 1R6F Reference Cigarette smoke. This study will provide the first published characterisation of chemical composition and *in vitro* mechanistic effects, in our multiple endpoint toxicity testing approach, of these particular p-HTP variants' aerosols, compared to 1R6F Reference Cigarette smoke.

2. Materials and methods

2.1. Test articles and stick conditioning

The p-HTP device was used with two consumable (stick) variants, Regular and Menthol; these two stick variants were identical except for additional flavouring added to the Menthol variant. The p-HTP sticks were obtained directly from production and packs were stored at room temperature, sealed in portions per test, in airtight containers and protected from light. The 1R6F Reference Cigarette (Kentucky Tobacco Research and Development Center, University of Kentucky) was used as a comparator (stored frozen, sealed in the original packaging until conditioned). The p-HTP device and stick structure are illustrated in Figs. S1 and S2 (Supplementary information). Briefly, a rechargeable battery powered device, including a heating rod, is used with a consumable containing reconstituted tobacco. Upon device activation, the heating rod subsequently heats the tobacco portion of the consumable (from the inside outwards), producing an aerosol that is delivered to the consumer as they draw air through the filter. The p-HTP can operate at two different temperatures, 315 °C and 345 °C, both well below typical temperatures in combustible cigarettes (around 900 °C). The highest temperature setting (345 °C) on the device was used for this study. The 1R6F Reference Cigarettes and p-HTP Regular sticks were conditioned for at least 48 h at 22 ± 1 °C and 60 ± 3% relative humidity, according to International Organization for Standardization (ISO) Guideline 3402 ISO (1999) prior to smoke/ aerosol generation. To preserve stick flavouring content, p-HTP Menthol sticks were

conditioned for 24 h only at 22 ± 1 °C and 60 ± 3% relative humidity prior to aerosol generation.

2.2. Smoke/ aerosol generation

For the Ames test, the 1R6F Reference Cigarette smoke was generated in accordance with ISO 3308 ISO (2012) (35 ml puff volume, 2 s puff duration, 60s puff interval, bell shaped puff profile, no ventilation blocking). For the chemical analysis of smoke/ aerosol, MN assay, NRU assay and generation of bubbled phosphate buffered saline (bPBS) stocks, 1R6F Reference Cigarette smoke was generated using the ISO 20778 smoking regime ISO (2018b) (formerly known as the Health Canada Intense (HCI) regime) (55 ml puff volume, 2 s puff duration, 30s puff interval, bell shaped puff profile, ventilation blocking). For all assays, p-HTP aerosols were generated using a modified ISO 20778 regime (55 ml puff volume, 2 s puff duration, 30s puff interval, bell shaped puff profile), with no ventilation blocking. At present, no ISO puffing regimes for HTPs have been published, therefore in the absence of an ISO approved method, this modified ISO 20778 regime was used. Furthermore, in the CORESTA technical report, 'Heated Tobacco Products (HTPs): Standardized Terminology and Recommendations for the Generation and Collection of Emissions' CORESTA Heated Tobacco Products Task Force (2020), it is stated that: '*Health Canada Method T-115:2016 and ISO 20778:2018 both require filter ventilation holes to be occluded during testing. The rationale for this is that users may block these holes with their lips or fingers during normal consumption and subsequently affect smoke yields. Vent blocking should be applied to eHTP consumables only if (a) ventilation holes in the product 'filter' section can be occluded in normal use and (b) vent blocking does not compromise the operation of the device (for example, air inlet holes in the device are not 'vents' and must not be occluded in testing) (Gee et al., 2018)*' (Gee et al., 2018; ISO, 2018b). Ventilation blocking was therefore not applied to the p-HTP sticks in this study as these are inserted into the device (not held) and as the ventilation holes are 4 mm from the heating device and 1.6 cm from the mouth-end of the stick, thus it is highly unlikely that consumer's fingers or lips would block these holes during product use. The differences in puff intervals between 1R6F (60s) and p-HTPs (30s) in the Ames test were due to excessive cytotoxicity with a shorter puff interval for 1R6F, however, due to the reduced toxicity of the p-HTPs in comparison, the 30s puff interval for these products was deemed suitable.

For air-liquid interface (ALI) exposures (NRU and MN assays), exposure was carried out using the Smoke Aerosol *In Vitro* System (SAEIVS) (described by Rudd et al. (2020) and Wieczorek et al. (2020)). Briefly, in respective machine runs, the p-HTPs or 1R6F were set up within smoking chambers from which puffs of the products were drawn, using the smoking regimes described above. Aerosol/smoke was drawn through tubing into a mixing pump, then into dilution syringes, where fresh filtered air can be used to dilute if necessary. The smoke/ aerosol is then drawn into exposure chambers containing cell culture plates (24 or 96 well format) and delivered using a distribution plate with a port above each well. Pre-specified numbers of puffs were delivered, and dose responses were achieved using a sliding lid to cover specific rows of the plate. After each puff, the smoke/ aerosol was drawn out of the wells/ chambers *via* an exhaust. All components were thoroughly cleaned between each product alongside regular cleaning as standard.

In the case of the Ames assay, whole smoke/ aerosol was bubbled through the bacterial cultures, achieved using the Vitrocell VC 10 S-Type Smoking Robot (Vitrocell, Germany).

Bubbled PBS (bPBS) solutions were generated for use in the scratch wound assay and HCS using the Vitrocell VC 10 S-Type smoking robot. Smoke/ aerosol extracts were trapped by bubbling the smoke or aerosol through 10 ml of PBS in each of three in-line glass impingers (total PBS volume 30 ml), and these solutions were pooled to create master stock solutions equating to concentrations of 4.5 puffs/ml (total 135 puffs/30 ml) for the p-HTP variants and 1.86 puffs/ml (total 56 puffs/30 ml) for 1R6F.

2.3. Smoke/ aerosol chemistry analysis

Methodology for the chemical analysis of the whole and bPBS extracted smoke/ aerosol can be found in the Supplementary information.

2.4. Cytotoxicity assessment

Cytotoxicity of the whole smoke/ aerosols of the test articles was measured using the neutral red uptake (NRU) assay with BEAS-2B human bronchial epithelial cells (ECACC 95102433; Lot No. 06C035). Cell stocks were stored in liquid nitrogen until use, and cultures checked for the absence of mycoplasma. The BEAS-2B cells were cultured in Epithelial Cell Growth Medium (Promocell #C-21060) with Supplement Mix (Promocell #C-39165) added. Only cells between 3 and 20 passages after thawing were used for the experiments. Prior to whole smoke/ aerosol exposure, 100 µl of cell suspension was seeded at a cell density of $0.5x10^4$cells/ml into the inner 60 wells of 96 well round bottomed collagen I coated plates and incubated at 37 °C and 5% CO_2 for 20 ± 3 h. The collagen I coated plates were prepared by adding 25 µl of collagen I solution (20% PureCol® EZ Gel, 2% 1 M HEPES buffer and 78% cell culture medium; final collagen I concentration, 0.1%) to each well of the 96 well plate. Directly prior to exposure, medium was removed from the cells by suction and reverse plate centrifugation for 10s at 70 ×*g* to guarantee complete and homogenous removal of medium from the wells for the ALI exposures. Cells were then exposed at the ALI to increasing puff numbers of fresh whole smoke/ aerosol using the SAEIVS according to the puffing regimes described above (*Smoke/ aerosol generation* section). The final exposure range for 1R6F smoke (diluted either 1:15 or 1:20 with air) was 0–0.6 puffs (corrected for dilutions) and 0–27 puffs for p-HTP Regular and p-HTP Menthol aerosols (undiluted). Cells were exposed for no >15 min, and following exposure 200 µl of fresh medium was added to each well and cells were incubated for 65 ± 2 h. Following this incubation period, the incubation medium was replaced by 200 µl fresh medium containing neutral red dye for 3 h, during which time, dye was taken up by viable cells. After washing and lysing of the cells, absorbance (540 nm) in the wells was then measured using a Tecan Sunrise plate reader, with absorbance directly proportional to the number of live cells present. From the absorbance values, mean relative cell viability compared to the values measured for control wells (0 puffs smoke/ aerosol) was calculated for each test concentration. Three biological replicates, each with two technical replicates, were carried out for each test article. Validation of the effects in the NRU assay of control exposure at the ALI compared to the outcomes in cells that remained within medium is demonstrated in Fig. 2.

2.5. MN assay

V79 Chinese hamster lung fibroblast cell (ECACC 86041102) stocks were stored in liquid nitrogen until use, and cultures were checked to confirm the absence of mycoplasma. Only cells between 3 and 20 passages after thawing were used for the experiments. Cells were cultured in Dulbecco's Modified Eagle's Medium supplemented with 10% fetal bovine serum. Prior to exposure, 250 µl of the medium was added to each well of a 24 well plate, and polycarbonate transwell inserts (0.4 µm pore membrane; 140,620, Nunc) were added to these. Four hundred microlitres of V79 cell suspension was seeded at a density of $1x10^5$cells/ml into each insert, then plates were incubated at 37 °C and 5% CO_2 for 20 ± 2 h. Directly prior to whole smoke/ aerosol exposure, the inserts were transferred to fresh plates containing 250 µl of medium/ well supplemented with HEPES buffer (final concentration, 20 mM) and the apical medium was removed. Whole smoke/ aerosol exposures were subsequently carried out at the ALI, and cells were exposed to increasing puff numbers of whole smoke (diluted)/ aerosol (undiluted), achieved using the sliding plate cover within the SAEIVS exposure chamber. The exposure range for whole p-HTP aerosol was 0–36 puffs (+/-S9), and for

1R6F smoke, 0–2.5 puffs +S9 (corrected for dilution of 1:4 with air), or 0–1.67 puffs –S9 (corrected for dilution of 1:6 with air). Exposures were no longer than 20 min. Following exposure, inserts were transferred to plates containing 250 µl of fresh basal medium. For metabolic activation of whole smoke/ aerosol components, S9 mix containing an S9 fraction derived from Aroclor 1254 treated male Sprague-Dawley rats (10% *v*/v S9 fraction, 90% v/v REGENSYS A, 1.3 mM NADP; TRINOVA Biochem) was added to medium (final concentration, 1% S9) and 250 µl of this added to each insert immediately following exposure. Following a 3 h incubation, the S9 mix was removed from the cells and 400 µl fresh medium was added. Cells were then incubated for a 20 ± 2 h recovery period. For exposed cultures without metabolic activation, 400 µl of fresh medium was added into the inserts immediately following exposure and cells were incubated for 20 ± 2 h.

Following this incubation period, cells were detached from the inserts using Accutase® and counted using the Scepter™ Cell Counter (Millipore) to determine cell density for microscope slide preparation and cell counts for relative cell count (RCC), relative population doubling (RPD) and relative increase in cell count (RICC) calculation, to assess treatment-induced toxicity. Cell suspensions were fixed to slides by spinning at 380 ×g for 5 min using the Cytospin and applying further spin cycles for drying. Fixative solution was then applied to the slides (methanol: glacial acetic acid: 37% formaldehyde: water 150:18.5:1:30.5), followed by one rinse in methanol, and slides were allowed to air dry. Prior to slide analysis, cells were stained with 1 µg/ml DAPI in mounting medium (Vectashield, H-1000). Slides were analysed using the automated Metafer system with a Z2 microscope (Zeiss). At least 1000 cells per replicate treatment were scored for MN according to pre-programmed Metafer parameters, based on the criteria described by Fenech (1993). For each test article, two biological replicates each with two technical replicates were carried out for each of the +/-S9 treatments. The assay was carried out in accordance with OECD TG 487 (OECD, 2016). The positive controls used in the assay are detailed in the Supplementary information (Table S4).

2.6. Ames bacterial reverse mutation assay

The TA98 and TA100 bacterial strains (Trinova Biochem GmbH) were used in this study. Sixteen hour Nutrient Broth No.2 (OXOID) cultures were prepared by inoculating 40 ml of medium with 0.7 ml of 6 h pre-culture in a 100 ml Erlenmeyer flask with one bacterium-coated CRYO-glass bead. These were incubated overnight at 37 °C, shaken at 120 rpm. Following this, the respective bacterial suspensions were pooled into 120 ml suspensions (3x40ml) and centrifuged at 1800 ×*g* for 10 min. The supernatant medium was removed and cells resuspended in 12 ml of Dulbecco's PBS (DPBS) (Ca^{2+} and Mg^{2+} free). Ten millilitres of this suspension was added to a glass tube, which was inserted into an impinger connected to the Vitrocell VC 10-S Smoking Robot. Smoking/ aerosol generation regimes were as described above (Smoke/ aerosol generation section), and exposure to the test article smoke/ aerosols was carried out at room temperature (RT) and protected from direct light.

The bacterial suspensions were exposed to increasing puff numbers of fresh whole smoke/ aerosol using the Vitrocell VC 10-S Smoking Robot according to the puffing regimes described previously in this section. During exposure, 350 µl of bacterial suspension was taken at regular intervals. For each repeat (petri dish), 50 µl of the suspension and added to sterile 15 ml tubes, followed by 0.5 ml of 5% S9 mix or 0.5 ml 0.2 M phosphate buffer. Two millilitres of top agar (45 °C) was then added to these. This mixture was then poured onto Vogel-Bonner agar plates (3 plates +S9, 3 plates –S9 per biological replicate), and the top agar was distributed by tilting/ rotating. When the top agar had solidified, plates were inverted and incubated at 37 °C for 48 h. Following this, the total number of revertant colonies per plate was counted automatically using the Synbiosis ProtoCOL SR Automatic Colony Counter (Meintrup-DWS). Validity of the results was checked against the following criteria: mean negative control counts fell within the historical range, positive controls induced clear increases in revertant colonies (+/-S9), no >5% of plates were lost due to contamination/ other unforeseen circumstances. Any observed pinpoint colonies were excluded from the analysis. Two biological replicates, each with three technical replicates, per strain (+ or –S9) were carried out for each test article. The assay was carried out in accordance with OECD TG471 (OECD, 2020). Positive controls are detailed in the Supplementary information (Table S4).

2.7. Scratch wound assay

Human umbilical vein endothelial cells (HUVECs) (pooled from several donors; C-12203/ C-12253, Lot No. 422Z021, PromoCell®; CoA: https://promocell.com/wp-content/uploads/product-information/coa/422Z021.pdf) were maintained in Endothelial Cell Growth Medium 2 (C-22011, PromoCell) supplemented with Growth Medium 2 SupplementMix (C-39216, PromoCell), at 37 °C and 5% CO_2. Only cells between 3 and 20 passages after thawing were used for the experiments. For the scratch wound assay, cells were seeded into 96 well ImageLock™ microplates (4379, Essen BioScience) at a density of 2.5×10^4 cells/well and allowed to reach 100% confluency (18 ± 1 h). The WoundMaker™ (Essen BioScience) was then used to make an artificial scratch (width 700-800 µm) in the cell layer in each well. Cells were then exposed to increasing concentrations (%) of bPBS in medium (data is plotted on a puffs/ml basis to reflect the puff-wise plotting in regulatory toxicity battery; nicotine equivalent details can be found in the Supplementary information (Table S3.2)). Test concentrations were applied in 8 wells/ plate, with 7 non-zero test concentrations/plate. Exposure was carried out over 30 h and cell migration was observed *via* scanning analysis every 2 h with the IncuCyte® ZOOM system (Essen BioScience) (physiological conditions: 37 ± 1 °C, 5 ± 0.5% CO_2, >85% humidity). Positive control, cytochalasin D (CAS #22144–77-0) (Sigma-Aldrich; #C2618), was applied at a concentration of 0.35 µM and PBS was used as a negative control (10% PBS in medium).

Image-based analysis of each well was carried out (example images can be found in Fig. 6a). Masking was used to differentiate cell occupied and cell free areas, with the initial scratch wound mask of importance for reference of changes from the initial timepoint. A second analysis was then carried out using an algorithm (Essen BioScience) which calculated the density of the cell region and the wound region, defined by the relevant masks. This output was used in the equation to calculate relative wound density (RWD) at a given timepoint:

$$\%RWD_t = 100^* \frac{w_t - w_{t0}}{c_t - w_{t0}}$$

where w = density of wound region; c = density of cell region; t = time; t0 = time, 0 h.

This equation accounts for the background density of the wound at the initial timepoint (0 h) and expresses the wound region density as a function of the cell region density. At 0 h, the RWD is 0%. RWD was plotted against time for each experimental treatment and a value obtained for the time taken for the initial wound to close to 50% of its original area (RWD50) was calculated. RWD50 for each test concentration was plotted and the slope (sRWD50), corresponding to the rate of wound healing, determined.

The assay was considered as valid if the mean RWD50 of the negative control fell within the normal/ historical range, the positive control induced clear inhibition of the migration (wound healing) rate and no >5% of test wells were lost due to unforeseen events (*e.g.*, out of focus situations). In addition to these conditions being met, the test article was considered to have an inhibitory effect on wound healing if sRWD increased significantly compared to the negative control value, a linear dose response was achieved and positive responses were reproducible. Assays were performed in triplicate (three independent test days).

2.8. High content screening

Normal human bronchial epithelial (NHBE) cells from a single donor (60 year-old Caucasian male) were obtained from PromoCell GmbH (C-12640/ C-12641, Lot No. 424Z013; CoA: https://promocell.com/wp-content/uploads/product-information/coa/424Z013.pdf) and maintained at 37 °C and 5% CO_2 in Airway Epithelial Cell Growth Medium (PromoCell, C-21060) supplemented with SupplementMix (Promocell, C-39165) containing bovine pituitary extract 0.004 ml/ml, epidermal growth factor (10 ng/ml), insulin (5 μg/ml), hydrocortisone (0.5 μg/ml), epinephrine (0.5 μg/ml), triiodo-L-thyronine (6.7 ng/ml), transferrin, holo (10 μg/ml), and retinoic acid (0.1 ng/ml). Only cells between 5 and 12 passages after thawing were used for the experiments.

For experimentation, cells were seeded into black walled 96-well microplates (Corning, product #3904) at a density of 15×10^3 cells/well (100 μl of 15×10^4 cells/ml suspension) and incubated overnight at 37 °C and 5% CO_2. The following day, 25 μl of 5-fold concentrated bPBS pre-dilutions were added to the cell culture medium resulting in increasing dose levels of the bPBS stocks (% in medium) (negative control 10% bPBS; 5 non-zero dose levels) ($n = 6$ technical × 3 biological replicates). The p-HTP aerosol bPBS stocks were tested up to 10% in the cell culture medium and following one replicate with excessive cytotoxicity at a maximum 1R6F smoke bPBS concentration of 6%, the maximum concentration here was reduced to 4% for the subsequent replicates. Lower concentrations of bPBS stock were prepared by diluting with untreated PBS. Cells were exposed for 4 and 24 h for measurement of all HCS endpoints, except GSH, which was assessed following a 2 h treatment only. Positive controls were dissolved in PBS or dimethyl sulphoxide (DMSO) (FCCP, etoposide, additional negative control: 0.5% DMSO). Details of positive controls for each HCS endpoint can be found in the Supplementary information (Table S4). Treatments were not applied to wells on the outer edges of the plates to avoid edge effects.

Immunostaining was carried out for the ɣH2AX (mouse-anti phospho-histone H2AX (Ser139 clone JBW301; Cat. No. 05–636, Millipore) and NfκB (rabbit anti-NfκB (ab32536, Abcam) endpoints within wells in parallel. Cytochrome c (mouse-anti-cytochrome *c* antibody (ab110325, Abcam) and phospho-c-jun (rabbit anti-c-jun (phospho S36; ab32385, Abcam) were also detected in parallel. Following treatment, the supernatant was removed and cells were washed once with 100 μl of PBS. Cells were then fixed within the wells with 50 μl fixative (4% formaldehyde in PBS) for 15 min at RT. The fixative was then removed and cells washed twice with PBS. Following this, 50 μl of permeabilization buffer (0.1% TritonX100 in PBS) was added and cells were incubated with this for 15 min at RT before removal of the buffer and washing with PBS. Cells were then incubated with 50 μl of blocking buffer (3% BSA in PBS (*w/V*)) for 60 min at RT. Following this, the blocking buffer was removed and 50 μl of 1:500 dilutions in antibody buffer (0.1% Tween20 in blocking buffer) of the antibody pairs mentioned above were added to the relevant wells. Plates were then incubated overnight at 4 °C. The following day, the antibody buffer solution was removed and cells washed twice with PBS. Fifty microlitres of 1:500 dilutions of the appropriate fluorophore conjugated secondary antibodies (donkey anti mouse Alexa Fluor 647 (ab181292, Abcam) or goat anti-rabbit Alexa 488) in antibody buffer plus DAPI (to counterstain the cell nuclei) was incubated with the cells for 60 min at 37 °C. This was then removed and cells were washed twice with PBS. Fifty microlitres of fresh PBS was then added to each well for the subsequent HCS analysis.

For the GSH depletion assessment, following 2 h of treatment with the bPBS test articles, cells were rinsed with 100 μl of DPBS (with Mg^{2+} and Ca^{2+}). ThiolTracker™ Violet dye (Product No. T10096, Invitrogen) was diluted 1:1000 in DPBS (Mg^{2+}, Ca^{2+}) and supplemented with 1:1000 diluted 1 mg/ml Hoechst solution for DNA staining. One hundred microlitres of this solution of this was added, prewarmed, to each well and cells incubated for 30 min at 37 °C. The staining solution was then removed and replaced with 100 μl of 4% formaldehyde in PBS solution, followed by fixation with this for 30 min at RT. Cells were then rinsed with PBS and 100 μl of fresh PBS added for the subsequent HCS analysis.

For MMP assessment, the Mitochondrial Health Kit (Product No. H10295, Invitrogen) was used. Fifty microlitres of the mitochondrial health stain solution was added to each well and incubated for 30 min at 37 °C and 5% CO_2. This was then removed and replaced with 100 μl of fixative with Hoechst counterstain, with which cells were incubated for 15 min at RT. Cells were then washed twice with PBS and then 200 μl of fresh PBS was added for the subsequent HCS analysis.

The HCS analysis was carried out using the Thermo Scientific ArrayScan XTI High Content Analysis Reader. On the analysis software, masks were created to outline areas of interest within the wells. Depending on the location of the marker of interest, masks were set to analyse the entire cell, the nucleus, or the cytoplasm. Details of the regions analysed for each HCS endpoint can be found in the Supplementary information (Table S6) and example images are shown in Fig. 7. Counts of the valid objects in a defined area per well (20 fields per well) were used for cytotoxicity (cell count) measurement. Fluorescence intensity data obtained from the analysis was in arbitrary units (AU), which for each replicate were normalised to negative control AU levels and expressed as a fold change. Variability of the negative control data was determined and the median absolute deviation (mad) (mad = 1.4826*median(|X-median(X)|)) was calculated for each marker. A three-fold change in mad defines the upper and lower background limits in determining relevant effects. This measure was adapted for minimum effect concentration determination in the Gladiatox R-module which was developed by Belcastro et al. (2019). Hence, in the present study the following criteria were used to define a relevant response: (i) the dose response exceeded the upper or lower background limit; (ii) the dose response exhibited a slope statistically different from zero as calculated in an analysis of variance (ANOVA) trend test analysis; (iii) the values achieved statistically significant differences to the negative control.

All reagents, unless specified as from elsewhere, were purchased from Sigma-Aldrich (Germany).

2.9. ToxPi data plotting

Selected data generated from the HCS analysis was plotted using the ToxPi software (Reif et al., 2013) to obtain visual plots of this data (Chapman et al., 2020). Data was prepared in csv. Format and included data values for each endpoint, timepoint and test article, maximum response values recorded to all three test articles pooled for each endpoint (including all timepoints) and the minimum value observed. Minimum values were set to a onefold change in response and data was expressed as fold change compared to background (onefold). In cases of a decrease in signal response (downward change), values were inverted (1/value) to allow for visualisation on the ToxPi plot. Here, the data selected for plotting was that from low (1R6F, average 1.75 μg/ml), equivalent (all test articles, average 7 μg/ml) and high (p-HTP, average 17 μg/ml) nicotine concentrations achieved within the cell culture medium. Scores generated from the plotted data were also calculated to obtain a potency ranking for the test articles, using the sum of values plotted on the ToxPis for all endpoints minus the sum of one-fold values.

2.10. Statistical analyses

Statistical analyses were carried out using GraphPad Prism version 8.4.3.

Neutral red uptake: EC50 (exposure concentration required to elicit 50% maximal cytotoxicity) and EC20 (exposure concentration required to elicit 20% maximal cytotoxicity) values were calculated using a Hill function analysis. Cytotoxicity was classed as significant if >EC20 was achieved in all three biological replicates. For the preliminary comparison of control cultures in the NRU assay under ALI and medium submerged conditions, a two-way ANOVA with a Tukey's multiple

comparisons test was carried out.

Micronucleus assay: MN frequency in treated samples were compared to the corresponding negative control populations with a Chi-square analysis to test for significant increases above background MN levels on each test day. To obtain an indication of relative effects of the test articles to each other on a per puff basis, ECMN3 values were calculated (number of puffs required to increase MN frequency by three-fold above background) with non-linear regression using the pooled values of both technical replicates per dose level.

Ames test: The test articles were considered mutagenic if reproducible two-fold or higher increases in revertant colonies, compared to negative control, were achieved at three or more test concentrations, in a linear manner. The data was tested with a non-threshold linear model and Dunnett's test.

Scratch wound assay: A one-way ANOVA was initially performed to determine linearity of RWD50 responses with dose. A one-way ANOVA with post-hoc Dunnett's multiple comparisons test was then carried out to compare the RWD50 responses at each dose to the corresponding negative control. A simple linear regression was performed on the calculated RWD50 values against dose to determine the slope (sRWD50) of the response.

HCS: A one-sided ANOVA with a post-hoc Dunnett's test was used to determine statistical significance and evaluate dose response trends for the absorbance data each marker and test article.

3. Results

3.1. Smoke/ aerosol compositional comparison

Upon comparison of selected emissions in the 1R6F whole smoke and p-HTP whole aerosols, substantial reductions in all analytes, except TPM and water, as expected, were observed in the p-HTP aerosols, on a per puff basis. Further to this, 14 analytes were recorded as below limit of quantification (LOQ) in both p-HTP aerosols. Total estimated reductions for each chemical grouping (TSNAs, PAH, carbonyls, volatiles) are detailed in Table S1 (Supplementary information) and range from >90.12 to 97.13% reductions for the p-HTP Menthol variant and > 89.71 and 97.90% for the p-HTP Regular variant per puff, compared to 1R6F smoke. Table 1 details TPM collected, water and nicotine content of these and also smoke/ aerosol CO emissions. Whilst comparable masses of TPM were collected from the samples, for the p-HTPs, a greater proportion of this was water. Nicotine levels were around 2.5-fold lower per puff for the p-HTPs under machine puffing conditions. High levels of CO, as present in cigarette smoke, is an indicator of tobacco combustion (Cozzani et al., 2020), however, levels were substantially reduced in the p-HTP aerosols as expected given the tobacco is heated and not burned (98.6% for p-HTP Regular; 98.7 for p-HTP Menthol). Fig. 1 summarises the total reductions for each chemical grouping and additionally in the WHO TobReg 9 list of priority toxicants proposed for reduction in cigarette smoke (Burns et al., 2008), which for p-HTP Regular were > 96.23% reduced and for p-HTP Menthol >95.73% compared to 1R6F smoke. The heatmap illustrates the substantial reductions in toxicant levels observed, and it must also be noted that values for benzo[*a*]pyrene (B[*a*]P), 1,3-butadiene and benzene were below LOQ levels and were included at their respective LOQ values as a conservative estimate of reductions. This is also the case for the 14 analytes below LOQ in the total reduction estimates.

3.2. Cytotoxicity in the NRU assay

An initial comparison of the differences in responses of negative control Beas-2B cells used in the NRU assay under both ALI and submerged conditions was carried out to validate the use of ALI approach use in this study. No significant differences in negative control measurements were observed between the conditions tested, providing validation for the ALI exposure approach. In the NRU cytotoxicity assessment following 1R6F whole smoke or p-HTP whole aerosol exposures, cytotoxicity was significant (>EC20 achieved) and clear dose responses were observed to all three test articles (Fig. 3), however, the number of puffs required to induce EC50 was on average 38-fold higher for the p-HTP aerosols compared to 1R6F smoke exposure. (See Figs. 2 and 3).

3.3. MN assay

Upon assessment of MN induction in V79 cells following exposure to whole smoke/ aerosol, significant responses were again observed at a much lower puff-wise exposure range to 1R6F than compared to the p-HTP aerosols, both in the absence and presence of S9 metabolising system. The lowest observed genotoxic effect level (LOGEL) for 1R6F was observed at an exposure of 1 puff +S9 and 0.66 to 1.33 puffs –S9, for p-HTP Menthol, 16 to 24 puffs +S9 and 24 puffs –S9 and p-HTP Regular 8 to 16 puffs +S9 and 16 puffs –S9 (Supplementary information, Tables S5.1-S5.12). Indicated using an ECMN3 comparison (Fig. 4), the 1R6F smoke demonstrated much greater potency than the p-HTP aerosols. The ECMN3 analysis also highlighted that the p-HTP Regular aerosol was 2.3-fold (+S9) and 1.7-fold (–S9) more potent than the p-HTP Menthol aerosol under the conditions of the test. Cytotoxicity/ cell count profiles for each test article can be found in the Supplementary information (Tables S5.1-S5.12); at the higher exposures for all test articles, substantial cytotoxicity, was induced (indicated on the plots in Fig. 4).(See Figs. 4 and 5).

3.4. Ames bacterial reverse mutation assay

The Ames bacterial reverse mutation test was carried out in two bacterial strains, TA98 and TA100 (both +S9 and –S9), demonstrated in combination to be responsive to HPHCs present in cigarette smoke (Rudd et al., 2020). In both strains, both in the presence and absence of S9, 1R6F smoke induced significant increases in revertant colonies with increasing numbers of puffs, and over a smaller puff-wise exposure range than tested with the p-HTPs. The p-HTP aerosols, however, did not induce significant increases in revertant colonies in either strain (+/− S9) under the conditions of test. Following the formation of non-revertant pinpoint colonies upon the first exposure replicate with p-HTP Menthol, indicating toxicity, the exposure range was reduced from

Table 1
Levels of total particulate matter (TPM) extracted from Cambridge filter pads used to trap 1R6F Reference Cigarette smoke/ p-HTP aerosol, respectively. Water and nicotine levels following this extraction are also expressed, along with carbon monoxide (CO) levels. Values are expressed on a per puff basis, and standard deviation (SD) of average measured values (1R6F: $n = 6$; p-HTP: $n = 5$) and the coefficients of variance (COV) are detailed for each analyte/ product. ‡Analyte detailed in WHO TobReg 9 list.

Analyte (mg/puff)	1R6F reference cigarette			p-HTP regular			p-HTP menthol		
	Average	*SD*	*COV (%)*	***Average***	*SD*	*COV (%)*	***Average***	*SD*	*COV (%)*
TPM	**4.41**	0.06	1.3	**4.63**	0.09	2.0	**5.15**	0.11	2.1
Water	**1.25**	0.04	3.4	**3.18**	0.49	15.3	**3.74**	0.08	2.2
Nicotine	**0.21**	0.00	1.2	**0.09**	0.01	5.9	**0.08**	0.00	4.0
CO‡	**3.32**	0.07	2.1	**0.05**	0.00	8.2	**0.04**	0.01	14.4

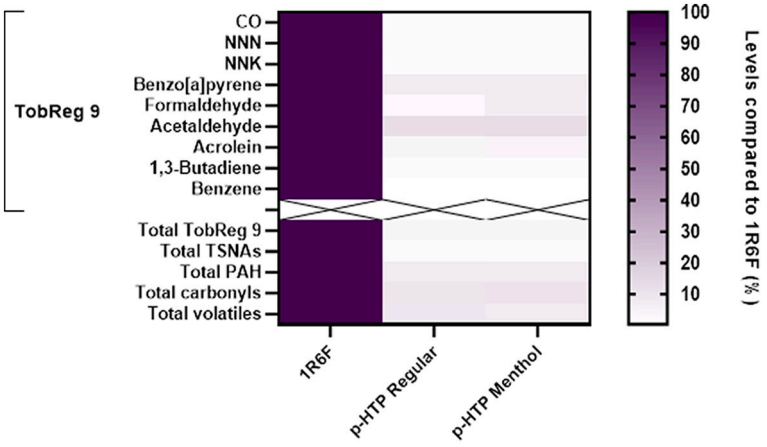

Fig. 1. Heatmap of the levels of selected analytes in the 1R6F Reference Cigarette and p-HTP aerosols, including the WHO TobReg 9 analytes and totals for the chemical classes measured, on a per puff basis. Full details of the compounds in each chemical class measured in this study can be found in the Supplementary information (Table S1). NNN = N-nitrosonornicotine; NNK = nicotine-derived nitrosamine ketone; TSNAs = tobacco specific nitrosamines; PAH = polycyclic aromatic hydrocarbon.

81 to 189 to 18–90 puffs. The non-revertant pinpoint colonies were not included in the slope analysis.

The bPBS stocks generated for the exposures in the scratch wound assay and HCS were analysed for the presence of eight carbonyls and nicotine to confirm trapping, and therefore *in vitro* exposure, of smoke/aerosol constituents. The eight carbonyls were selected based on a list detailed by Buratto et al. (2018) and are present on regulator HPHC lists (https://www.federalregister.gov/documents/2012/04/03/2012-7727/harmful-and-potentially-harmful-constituents-in-tobacco-products-and-tobacco-smoke-established-list). The nine analytes were detected in the bPBS stocks, detailed in the Supplementary information (Table S3.1), and the stocks were therefore deemed suitable for delivering exposures in these assays.

3.5. Scratch wound assay

Although significant increases in the slope of the RWD50 response with increasing bPBS puffs/ml concentration were observed in response to treatment will all three test articles, this response was reduced by around 60-fold on comparison of both p-HTP Menthol and p-HTP Regular aerosol bPBS to 1R6F smoke bPBS. In addition to this, the dose range over which this response was observed was 15-fold wider for the p-HTPs (0–0.45puffs/ml) compared to 1R6F (0–0.03puffs/ml). Therefore, 1R6F smoke bPBS was found to be a much more potent inhibitor of wound healing than either p-HTP aerosol bPBS. Additionally, in this endpoint, p-HTP Menthol and p-HTP Regular aerosol bPBS did not appear to demonstrate differences to each other in effects.

3.6. HCS

HCS was used to assess seven endpoints associated with cellular stress following exposure to smoke/aerosol bPBS (representative images of staining can be found in Fig. 7). Outcomes were plotted on a nicotine concentration in the cell culture medium (delivered *via* bPBS) basis, to provide a comparison of responses at equivalent nicotine concentrations (Figs. 8 and 9). Cell counts were greatly reduced (over a slightly lower nicotine concentration range) following exposure to the 1R6F smoke bPBS than with either p-HTP aerosol bPBS. The largest decreases in cell counts for all test articles were observed following the 24 h exposures. Cytochrome c, the release of which is associated with the early stages of mitochondria-initiated apoptosis, did not appear to be involved in the cells' responses to the p-HTPs' aerosol bPBS. However, following the 4 h treatment with 1R6F smoke bPBS, there was significant cytochrome *c* release observed, correlating with increasing dose. This response to 1R6F, however, was not present at the 24 h timepoint at the lower exposures and an increase in cytochrome *c* staining intensity was observed at the higher test doses, suggesting some adaptions in the surviving cell populations, involving other areas of cytochrome *c* activity. Mitochondrial respiratory function, indicated by the MMP measurement, was not affected by any of the test articles following 4 h exposure. The absence of effect of the p-HTPs' aerosol bPBS was also observed following 24 h exposure. At the higher 1R6F smoke bPBS concentrations tested, however, there were significant, dose dependent decreases in MMP following 24 h.

Phospho-c-jun, which has a role in many cell stress-related responses, including cell cycle arrest and regulation of apoptotic processes, was significantly increased in the cell nuclei with increasing doses following 4 h exposure to all three test articles. However, the response was much greater in magnitude to the 1R6F smoke-derived bPBS. This increase was sustained at 24 h in the case of the 1R6F exposure, with a decline correlating with decreased surviving cells at the top 1R6F exposure concentration. However, the effects were absent following this time in the case of the p-HTP aerosol samples. The NfκB translocation response was, again, much larger for the 1R6F smoke bPBS compared to the p-HTP aerosol bPBS, although all three test articles induced significant responses at both the 4 h and 24 h timepoints. Further to this, significant responses were observed at lower test concentrations of the p-HTP aerosol bPBS than seen with the other HCS endpoints, with a slight increase in effect of p-HTP Regular from 4 h to 24 h and a slight decrease in effect of p-HTP Menthol from 4 h to 24 h. Further to this, a decrease in GSH signal at 2 h correlated linearly with increasing 1R6F smoke bPBS dose, indicating the presence of oxidative stressors within this test article. In contrast, there was no change in GSH signal following exposure to the p-HTP aerosol bPBS samples at this timepoint. Phosphorylation of H2AX is an early indication of DNA double strand breaks, and following 4 h of exposure to the 1R6F smoke bPBS, there were significant increases in this signal at the higher concentrations tested. These large signals were also present following 24 h 1R6F bPBS exposure. The p-HTP Menthol aerosol bPBS did not appear to induce any DNA damage *via* double strand breaks above background levels, however, there was a significant signal at the top tested concentration following 24 h only for the p-HTP Regular sample, indicating possible low level secondary DNA damage.

In Fig. 9, the responses at selected nicotine concentrations in the cell culture medium were plotted as ToxPis to visualise and rank the cells' responses to the three test products in the HCS analyses. At an equivalent nicotine concentration of 7 μg/ml, 1R6F was the most potent test article, with a score >13 times higher than the p-HTP samples. Only at a nicotine concentration around 10 times higher for the p-HTPs compared to for 1R6F, potency scores for the three test articles became comparable.

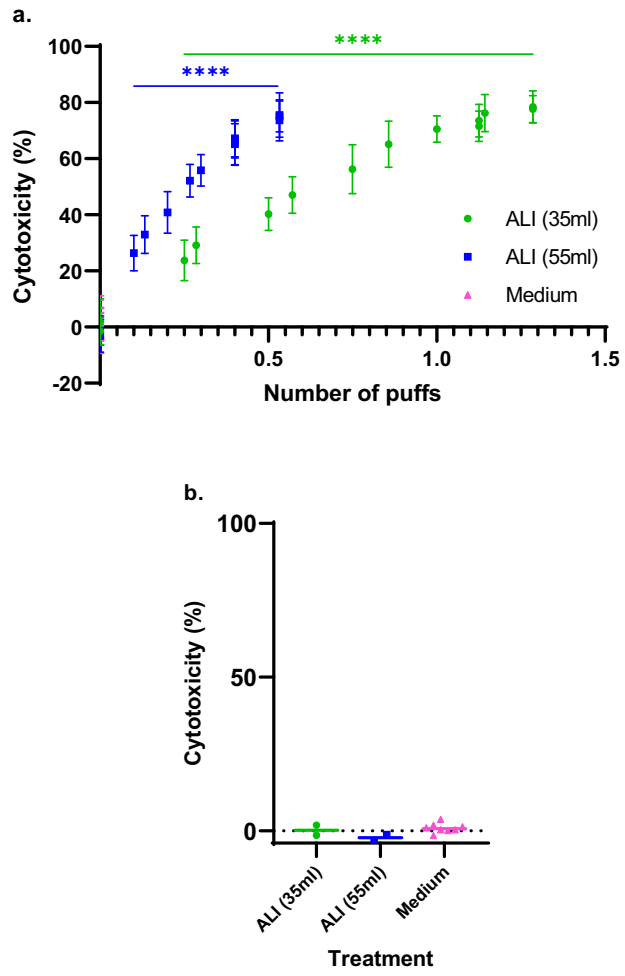

Fig. 2. An example of the responses of Beas-2B cells in the neutral red uptake (NRU) assay under different exposure conditions; NRU experiments were carried out as outlined in '*Cytotoxicity assessment*' (Materials and methods). (a) Cells were exposed at the air-liquid interface (ALI) (as in Fig. 3) to 1R6F reference cigarette smoke generated under 35 ml and 55 ml puff volumes, with the equivalent control wells exposed to 0 puffs of smoke, but with medium removed and therefore at the ALI, for the experimental duration. The 'medium' wells were within the same plate, but cells were covered in 200 μl medium/well, and foil to prevent smoke exposure, for the duration of the exposure. 1R6F dose responses are included to indicate the relative magnitude of the respective (35 ml and 55 ml experiments) cytotoxic dose responses. (b) Plot of the individual replicate means (symbols) and overall group mean (lines) values of responses of cells exposed either at the ALI or in medium (as described for (a)). Three replicates (days) were carried out for each of the two experiments (35 ml and 55 ml), with two technical replicates on each of these days. In (a) error bars represent standard deviation about average plotted values (symbols); significant responses in a two-way ANOVA with a Tukey's multiple comparisons test are denoted by asterisks: ****$p < 0.0001$. In (b) a two-way ANOVA with a Tukey's multiple comparisons test was carried out but no significant reproducible differences were observed between the three groups. (For interpretation of the references to colour in this figure legend, the reader is referred to the web version of this article.)

4. Discussion

4.1. Sample chemical analysis demonstrated reduced levels of HPHCs in p-HTP aerosols compared to 1R6F smoke

Upon assessment of selected analyte levels in the smoke/ aerosols generated from the test products, there were marked differences between the 1R6F smoke and p-HTP samples, with substantial reductions observed across the analyte categories. With a focus on the WHO TobReg9 priority toxicant list, these aggregated reductions for the p-HTPs were around 96%, which is consistent with the reductions seen with the HTPs tested and compared to 3R4F Reference Cigarette smoke by Forster et al. (2018). Included in this WHO TobReg9 list is CO, which may be considered a marker of tobacco combustion (Schaller et al., 2016). CO levels in the p-HTP aerosols were reduced by around 99% compared to levels in the 1R6F smoke, but generation of some low levels may be attributed to heating of other components found in the tobacco of HTPs, such as cellulose and hemicellulose (Cozzani et al., 2020; Eaton et al., 2018), or may be attributed to device heating (Bekki et al., 2017). These low levels of CO, however, indicate an absence of combustion in the p-HTPs consistent with the tobacco being heated and not burned. In slight contrast to some previous studies recording reductions, but still detectable levels, of B[*a*]P in HTP aerosols (Forster et al., 2018), we found B[*a*]P levels in the p-HTP aerosols to be below the LOQ, consistent with an absence of tobacco combustion and pyrolysis and still in line with other findings (Eaton et al., 2018). The presence of small levels of B[*a*]P in the HTP aerosols in previous studies may be attributed to low level tobacco pyrolysis or artefactual presence of PAHs, for example in the tobacco, and derived from environmental contamination during growing and curing processes (Cozzani et al., 2020). Detection of some other analytes, including NNN, NNK, formaldehyde and acetaldehyde, albeit at substantially lower levels than in the 1R6F smoke are unsurprising, however, as these begin to be generated within the range of 140–200 + ^{o}C (Forster et al., 2018) and this is line with previous reporting (Forster et al., 2018; Jaccard et al., 2017; Bekki et al., 2017). The water content in the p-HTP aerosols was to similar proportions as previously recorded in other HTP aerosols, generated as dehydration occurs at 100-300 °C in the tobacco heating process (Cozzani et al., 2020; Bentley et al., 2020). Furthermore, the comparable levels of TPM collected per puff from the p-HTP aerosols and 1R6F smoke can be attributed to the higher water content of the p-HTP aerosols making up a higher proportion of the TPM than in 1R6F smoke TPM. Nicotine levels in the p-HTP aerosols were around 2.5-fold lower per puff compared to in the cigarette smoke under machine puffing conditions. These lower levels of nicotine in HTP aerosols compared to cigarette smoke have been previously recorded (Farsalinos et al., 2017; Schaller et al., 2016) and has also been the case in clinical and consumer studies (Picavet et al., 2016; Jones et al., 2020). However, nicotine was found at higher levels in the p-HTP aerosols compared to the toxicants analysed, *i.e.*, the reductions were less for nicotine than the toxicants detected in the p-HTP aerosol (Table S1). This is in line with the THR potential of HTPs, in that nicotine delivery may be achieved for adult smokers, but in the presence of substantially fewer and lower levels of toxicants compared to combustible cigarette smoke. Based on previous HTP stick consumption data (Lüdicke et al., 2017; Roulet et al., 2017; Roulet et al., 2019; Farsalinos et al., 2019), it can be predicted that adult smokers would consume around 20 p-HTP sticks per day, with each p-HTP stick providing 8 puffs; this translates to 160 puffs per day. On comparison of the levels of the selected analytes measured here, emissions from one 1R6F stick (8.7 puffs) were more than double the emissions produced from 160 p-HTP puffs (20 consumed sticks), of either variant. The effects of this would be amplified on comparison of the number of puffs a typical adult smoker may take with the prediction for p-HTP (Jones et al., 2020). However, further investigation into user topography specific to the p-HTPs used in this study, and compared to commercial cigarette use, would need to be carried out to confirm these predictions. We have also assessed particle size distribution in the p-HTP aerosols using Andersen Cascade Impaction and the measured Median Mass Aerodynamic Diameter for the p-HTP aerosol particles was 0.8–1.1 μm, depending on flow rate (data not shown). The particles generated from the p-HTPs are comparable to those of combustible cigarette (3R4F; 0.8 μm) measured in a study by Schaller et al. (2016), indicating that the p-HTPs have comparable respirable profiles to combustible cigarettes, but with reduced exposure to toxicants.

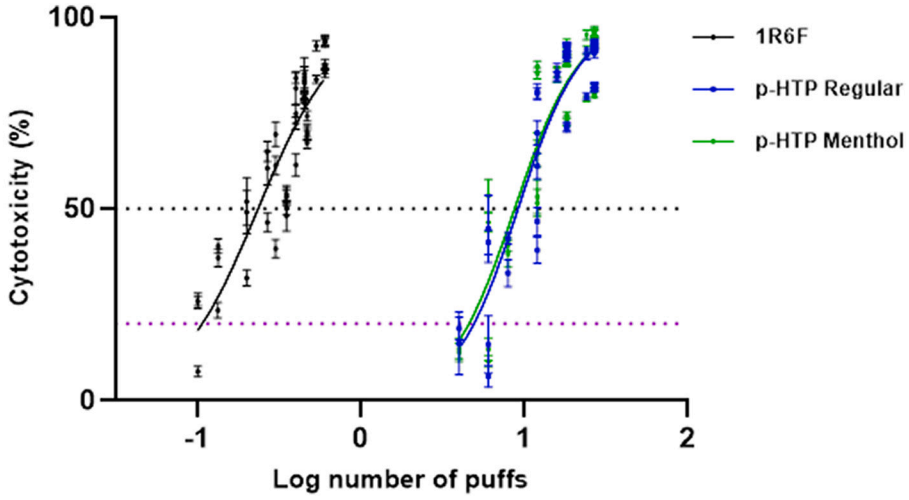

Product	EC20 (puffs)	EC20 equivalent nicotine exposure (mg)	EC50 (puffs)	EC50 equivalent nicotine exposure (mg)	Fold change EC50 compared to 1R6F Reference Cigarette
1R6F Reference Cigarette	0.106	0.02	0.234	0.05	1
p-HTP Regular	4.91	0.44	9.14	0.82	39.06
p-HTP Menthol	4.58	0.37	8.71	0.70	37.22

Fig. 3. Percentage cytotoxicity induced in the neutral red uptake assay (Beas-2B cells) with exposure to increasing numbers of puffs (log scale) of 1R6F Reference Cigarette whole smoke, p-HTP Menthol or p-HTP Regular whole aerosol. Fifty percent cytotoxicity (EC50) is marked with a black dotted line; 20% cytotoxicity (EC20), considered a statistically significant increase in cytotoxicity, is indicated with a pink dotted line; EC20 and equivalent nicotine levels are also detailed in the table. $n = 3$; error bars represent standard error of the mean (SEM). Due to the nature of the analysis, negative control (background) values are not plotted here. Exposures on a puff and nicotine basis can be found in the Supplementary information (Table S2.1). (For interpretation of the references to colour in this figure legend, the reader is referred to the web version of this article.)

Whilst the data presented here demonstrate substantial reductions in toxicants present in the p-HTP aerosols, our analysis was not as comprehensive as previous analyses, in terms of the number of analytes (Bentley et al., 2020; Schaller et al., 2016; Forster et al., 2018; Wang et al., 2021). However, on comparison of our selected analyte levels with those within such studies, it can be inferred that the p-HTP aerosols would likely exhibit similar results with a more comprehensive (non-targeted) aerosol screen. Future studies, including untargeted screening of the p-HTP aerosols are required to confirm this. Overall, our smoke/ aerosol chemistry analysis supports previous evidence of greatly reduced levels of a number of harmful chemicals in HTP aerosol compared to cigarette smoke, and this can be directly linked to the substantially reduced toxicity observed in a number of *in vitro* test systems.

For the scratch wound and HCS assays, smoke/ aerosol was trapped in PBS, and subsequently delivered to the cells within culture medium. This approach allows exposure in submerged cell cultures, and supported the assay designs, *i.e.*, 30 h scratch wound exposure period, 2-24 h HCS exposure periods with cells within medium. The bPBS was analysed for the presence of nicotine and eight carbonyls to ensure trapping and delivery of smoke/ aerosol constituents to the cells. Smoke/aerosol delivery *in vitro* using this aqueous extraction method is increasingly used as a means of exposure, however, it must be noted that this method will only deliver aqueous soluble constituents to the cell culture (Czekala et al., 2021; Simms et al., 2020; Smart and Phillips, 2021). HCS has been applied with TPM for HTP studies (Taylor et al., 2018; Gonzalez-Suarez et al., 2016), however, responses were not elicited to the degree seen with the p-HTP aerosol bPBS, perhaps due to the binding of hydrophobic compounds *in vitro* to the system components, or a lack of means to draw nicotine level equivalence between different studies. Future HCS analyses using cells exposed to whole aerosol would clarify effects of different aerosol fractions further, which would be a recommendation for future studies of this kind.

It is also worth noting that the aqueous nicotine concentrations applied within the cell cultures were thousands of times higher than physiological nicotine levels in adult smokers (10-50 ng/ml, Benowitz et al., 2009), and it can be assumed, therefore that the other measured chemical constituents would be present in comparably lower amounts in smokers' blood. Although nicotine levels in the whole smoke aerosol were measured, how this equates in terms of *in vitro* nicotine exposure and translatability to human exposures requires further elucidation; some preliminary work on this is outlined below (in '*Evaluation of the study and future direction*').

4.2. *p-HTP aerosols were consistently less toxic than 1R6F Reference Cigarette smoke in the single endpoint assays*

Upon comparison of the effects of two p-HTP variants' aerosols and 1R6F smoke samples in the three regulatory toxicity assays, the p-HTP aerosols were demonstrated to be significantly less potent than the 1R6F smoke. For example, on a (log) puff basis, EC50 values were around 38-fold greater for the p-HTP whole aerosols in the Beas-2B cell line than compared to 1R6F whole smoke. This is unsurprising, as HTPs have exhibited greatly reduced cytotoxicity compared to cigarette samples in a number of previous studies (Schaller et al., 2016; Jaunky et al., 2018; Murphy et al., 2018; Leigh et al., 2018). However, it has been demonstrated that different cell models can vary in their cytotoxic responses to HTP aerosol extracts *in vitro* (Davis et al., 2019). The application of multiple cellular models and mechanistic endpoints in the current study offers the advantage of a more comprehensive characterisation of the p-HTP variants.

Here, as there is currently no guidance or consensus on the most appropriate Ames strains for the assessment of HTPs, we selected two bacterial strains for the Ames reverse mutation test, TA98 and TA100, as these have demonstrated responsiveness to the chemicals found in cigarette smoke (Rudd et al., 2020; Williams et al., 2019). TA98 displays sensitivity to basic components of smoke including heterocyclic and aromatic amines, and this is complemented by the responsiveness of TA100 to carbonyls and its ability to differentiate tobacco products (Dillon et al., 1998; Rudd et al., 2020). These strains were deemed

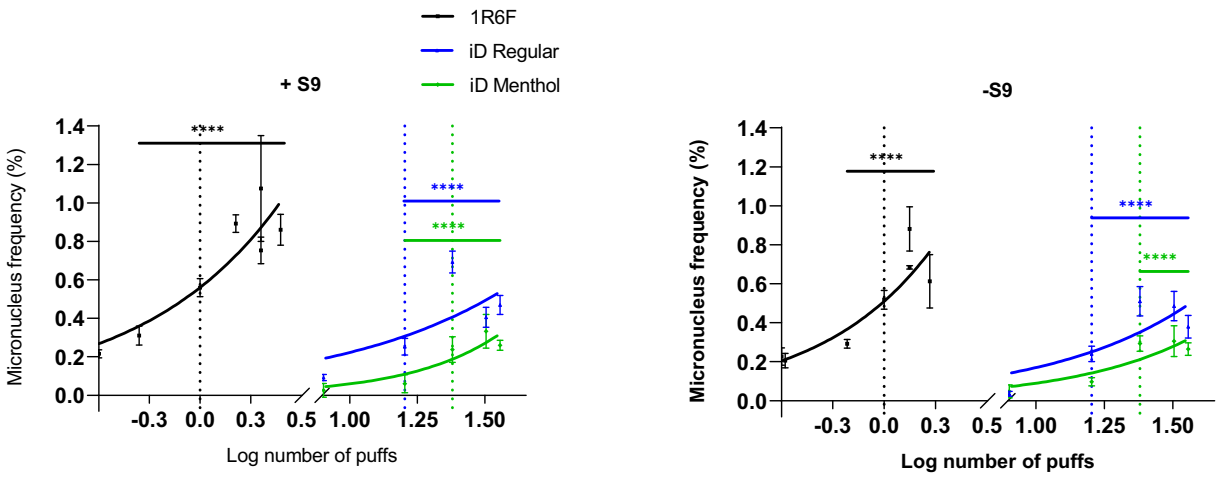

Product	ECMN3 (puffs)		ECMN3 equivalent nicotine exposure (mg)		Fold change compared to 1R6F Reference Cigarette	
	+S9	*-S9*	*+S9*	*-S9*	*+S9*	*-S9*
1R6F Reference Cigarette	1.6	1.3	0.34	0.27	1	1
iD Regular	12.6	16.6	1.13	1.49	8.0	12.8
iD Menthol	29.2	28.2	2.34	2.26	18.7	21.7

Fig. 4. Plot of background subtracted micronucleus frequency in V79 cells following exposure to increasing puffs (log scale) of 1R6F Reference Cigarette whole smoke or p-HTP Regular or p-HTP Menthol whole aerosol in either the presence (a) or absence (b) of S9 metabolising system. ECMN3 analysis was carried out using non-linear regression analysis (solid lines for each test item) to indicate the puff-wise exposure required to induce a MN frequency three times that of background levels for each test article. Equivalent nicotine exposure concentrations for the ECMN3 values are detailed in the table. Error bars represent SEM; $n = 2$ (x2 technical replicates each) for each test condition (in accordance with the conditions of the test). Due to the nature of the analysis, negative control (background) values are not plotted here. Statistically significant increases in MN frequency are denoted by asterisks (****$p \leq 0.0001$). Exposures on a puff and nicotine basis can be found in the Supplementary information (Table S2.2). Vertical dotted lines denote the exposures (log number of puffs) from which cytotoxicity above the OECD recommended threshold (55 ± 5%; measure: RPD) were induced for each test article (black: 1R6F, blue: p-HTP Regular, green: p-HTP Menthol); full cytotoxicity information can be found in the Supplementary information (Tables S5.1-S5.12). (For interpretation of the references to colour in this figure legend, the reader is referred to the web version of this article.)

suitable to test the p-HTP aerosols, therefore, due to the demonstrated commonality between the chemical compositions of HTP aerosols and cigarette smoke, albeit to different levels (Forster et al., 2018; Bentley et al., 2020; Bekki et al., 2017). Whilst significant, steep, increases in revertant colonies with increasing puffs of 1R6F smoke were observed in both strains (+/-S9), neither of the p-HTP samples were found to be mutagenic under the test conditions. This is consistent with many previous similar observations (Schaller et al., 2016; Breheny et al., 2017; Thorne et al., 2018; Godec et al., 2019). Initial testing of both p-HTPs was carried out to the exposure range of 81–189 puffs, however, this was reduced for subsequent replicates with p-HTP Menthol (to 18–90 puffs). This was due to the observation of toxicity-induced non-revertant pinpoint colonies at the higher test doses of 162 and 189 puffs. An explanation for this might be the sensitivity of bacterial strains to flavourings, for example, menthol (Trombetta et al., 2005), but these findings may not necessarily reflect a mammalian cell response.

Upon evaluation of MN induction following treatment of V79 cells with whole smoke/ aerosol (plus a recovery period), all three test articles induced significant increases in MN frequency, generally in a dose-dependent manner. Again, the puff-wise exposure range for the p-HTP aerosols (0–36 puffs) was much larger than the 1R6F smoke range (0–2.5 puffs), with LOGELs in the range of 0.66 to 1.33 puffs for the 1R6F smoke treatments and 8 to 24 puffs for the p-HTP treatments. The ECMN3 analyses also highlighted an 8 (+S9) to 12.8 (–S9)-fold difference between the p-HTP Regular aerosol and 1R6F and 18.7 (+S9) to 21.7 (–S9)-fold difference between p-HTP Menthol and 1R6F, with around 2-fold differences between p-HTP Regular and p-HTP Menthol responses. This again highlights the reduced toxicological effects of the p-HTP aerosols compared to cigarette smoke. However, the differences between the MN responses to the two p-HTP products may require some further elucidation. The increased MN frequencies induced by p-HTP Regular correlated with higher cytotoxicity of this product (Tables S5.5-S5.12, Supplementary information) within the assay V79 cell populations. On a per puff basis, there were no large differences between levels of measured aerosol constituents in the p-HTP Menthol and p-HTP Regular aerosols, therefore the response may be driven by additional aerosol components which were not measured here. As the p-HTP Menthol sticks also contain flavourings such as menthol, this may result in a dilution effect on these uncharacterised components of the aerosols, resulting in lower exposures to such constituents. Furthermore, MN responses in the presence of S9 were observed to be around 25% greater than in the absence of S9 for p-HTP Regular, suggesting the presence of DNA reactive metabolites.

The cell model used, V79, was selected as it has been extensively used and validated in *in vitro* MN testing (OECD, 2016) and is commonly used in NGP assessment (Thorne et al., 2020: Crooks et al., 2018; Wieczorek et al., 2020). However, it is of rodent and not human origin and therefore possesses deficiencies in the DNA damage response and exhibits greater sensitivity to test chemicals than human-derived cell lines (Fowler et al., 2012; Thorne et al., 2020; Thorne et al., 2019). Additional further investigation in the future into the effects of these p-HTP products on MN induction in human-derived cells *in vitro* will provide insight into any cell type-dependent differences. Of note in this study is the high cytotoxicity at the higher test doses of all test articles. Some caution must be taken in interpreting MN induction here, as the MN assay is based around MN counts in a dividing cell population, and

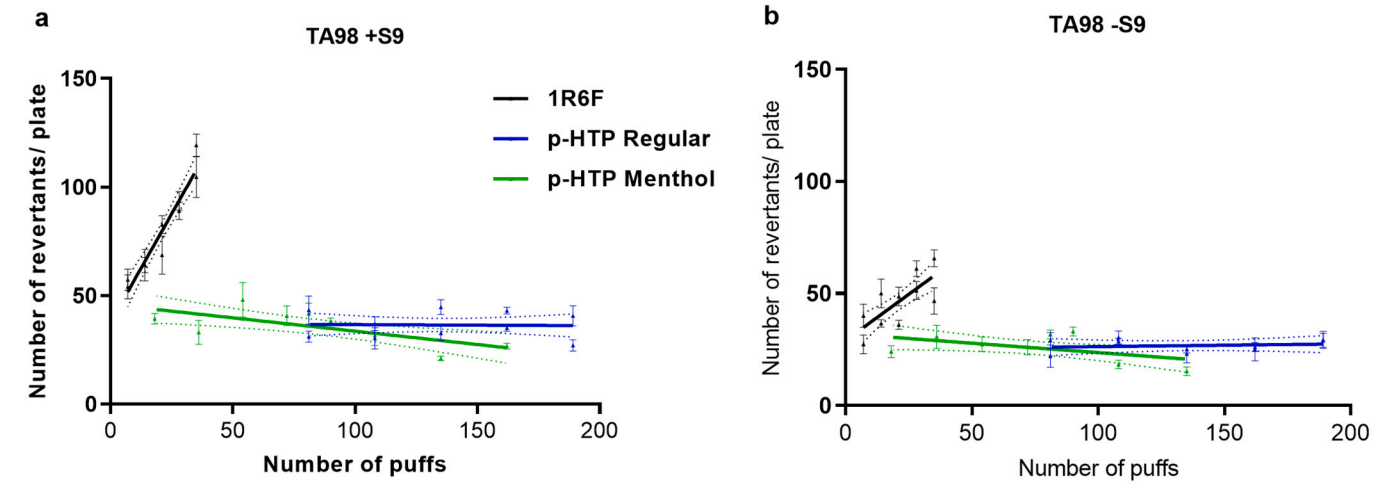

Product	TA98 response slope (significantly changed compared to 0?)		Fold change compared to 1R6F Reference Cigarette	
	+S9	*-S9*	*+ S9*	*-S9*
1R6F Reference Cigarette	2.00 (yes)	0.826 (yes)	1	1
p-HTP Regular	-0.00494 (no)	0.0124 (no)	405.0	66.9
p-HTP Menthol	-0.123 (yes*)	-0.0837 (yes*)	16.3	9.7

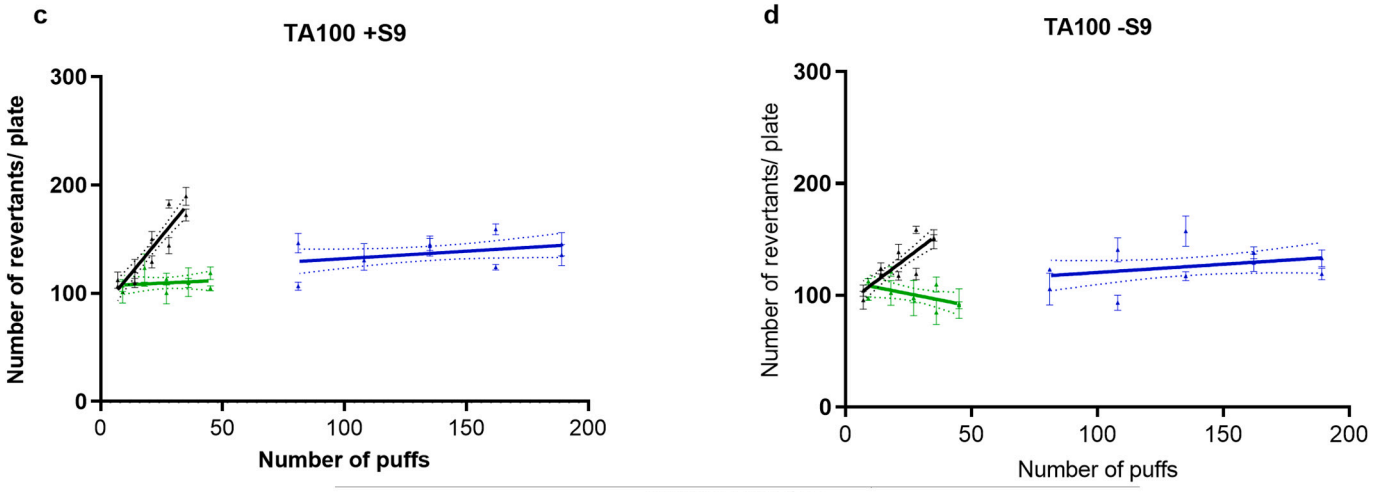

Product	TA100 response slope (significantly changed compared to 0?)		Fold change compared to 1R6F Reference Cigarette	
	+S9	*-S9*	*+ S9*	*-S9*
1R6F Reference Cigarette	2.74 (yes)	1.702 (yes)	1	1
p-HTP Regular	0.106 (no)	0.148 (no)	25.9	11.5
p-HTP Menthol	0.0658 (no)	-0.446 (no)	41.7	3.7

Fig. 5. Average number of revertant colonies per plate from either TA98 (a, b) or TA100 (c, d) bacterial strains exposed to increasing numbers of puffs of 1R6F Reference Cigarette smoke, p-HTP Regular or p-HTP Menthol aerosol in either the presence (a, c) or absence (b, d) of S9 metabolising system. n = 2 (x3 technical replicates each (6 for negative controls)) for each test condition (in accordance with conditions of the test); error bars represent SEM. Linear regression analysis was applied to the responses to each test article (solid trendlines) and the slope calculated; dotted lines represent the 95% confidence intervals about the slope. *significant but negative slope compared to control. Due to the nature of the analysis, negative control (background) values are not plotted here. Exposures on a puff and nicotine basis can be found in the Supplementary information (Tables S2.3 and S2.4).

above the toxicity thresholds detailed in OECD TG 487 (OECD, 2016), and cytotoxic artefacts may result in misleading MN counts. However, including the MN values at higher toxicities for all test articles allowed a better modelling for calculation of the ECMN3.

Cardiovascular disease is associated with cigarette smoking: constituents from the smoke reportedly cause oxidative stress which can result in endothelial damage, and can also impair the subsequent repair of this, leading to the inflammatory processes associated with atherosclerosis development (Fearon et al., 2012; Fearon et al., 2013; McQuillan et al., 2015; Taylor et al., 2017). Here, the scratch wound assay was used to assess HUVECs' wound healing capacity with exposure to the test articles, and with increasing exposure concentrations, 1R6F smoke demonstrated steep inhibition of wound healing potential, and across a ten-fold lower concentration range than tested with the p-HTP aerosol samples. There were small increases in inhibition with increasing dose for the p-HTP aerosols, and the slope of these responses

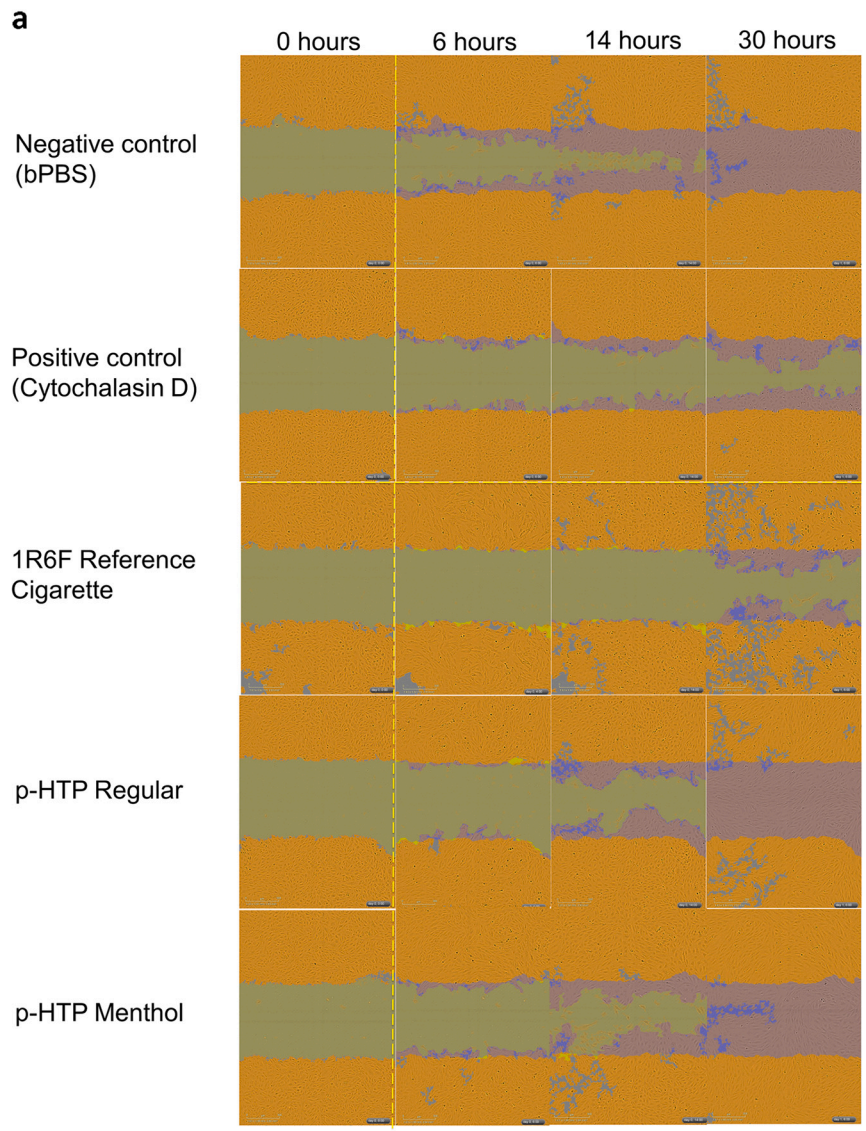

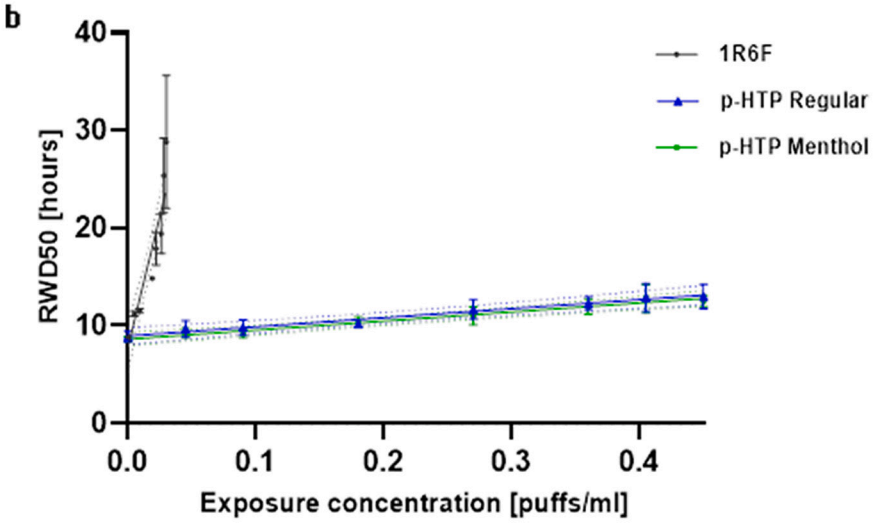

Product	RWD50 slope (significantly increased compared to 0?)	Fold change compared to 1R6F Reference Cigarette
1R6F Reference Cigarette	537.2 (yes)	1
p-HTP Regular	9.3 (yes)	57.8
p-HTP Menthol	9.3 (yes)	57.9

Fig. 6. (a) Phase contrast images illustrating scratch wounded cell cultures over the assay period (30*h*). Cells were wounded then the test articles added at 0 h. The different colours represent the masks used to calculate relative wound healing: green = scratch area (no cells); orange = original cell populated area following scratch wounding; purple = area of cells populating original wound area; blue: cell-free area (following cell migration). (b) Time taken for scratch wounded HUVEC monolayers to repopulate 50% of the original wound area (relative wound density 50% (RWD50)) at increasing puff/ml doses of 1R6F Reference Cigarette smoke, p-HTP Regular aerosol or p-HTP Menthol aerosol bPBS. The slope of the responses (obtained using a linear regression analysis) are indicated by the solid lines; dotted lines represent 95% confidence about the slope. Data is from three replicate days (with 8 cell culture wells per dose per replicate); error bars represent SEM. Nicotine concentrations corresponding to the puffs/ml exposures for each test article can be found in the Supplementary information (Table S3.2). (For interpretation of the references to colour in this figure legend, the reader is referred to the web version of this article.)

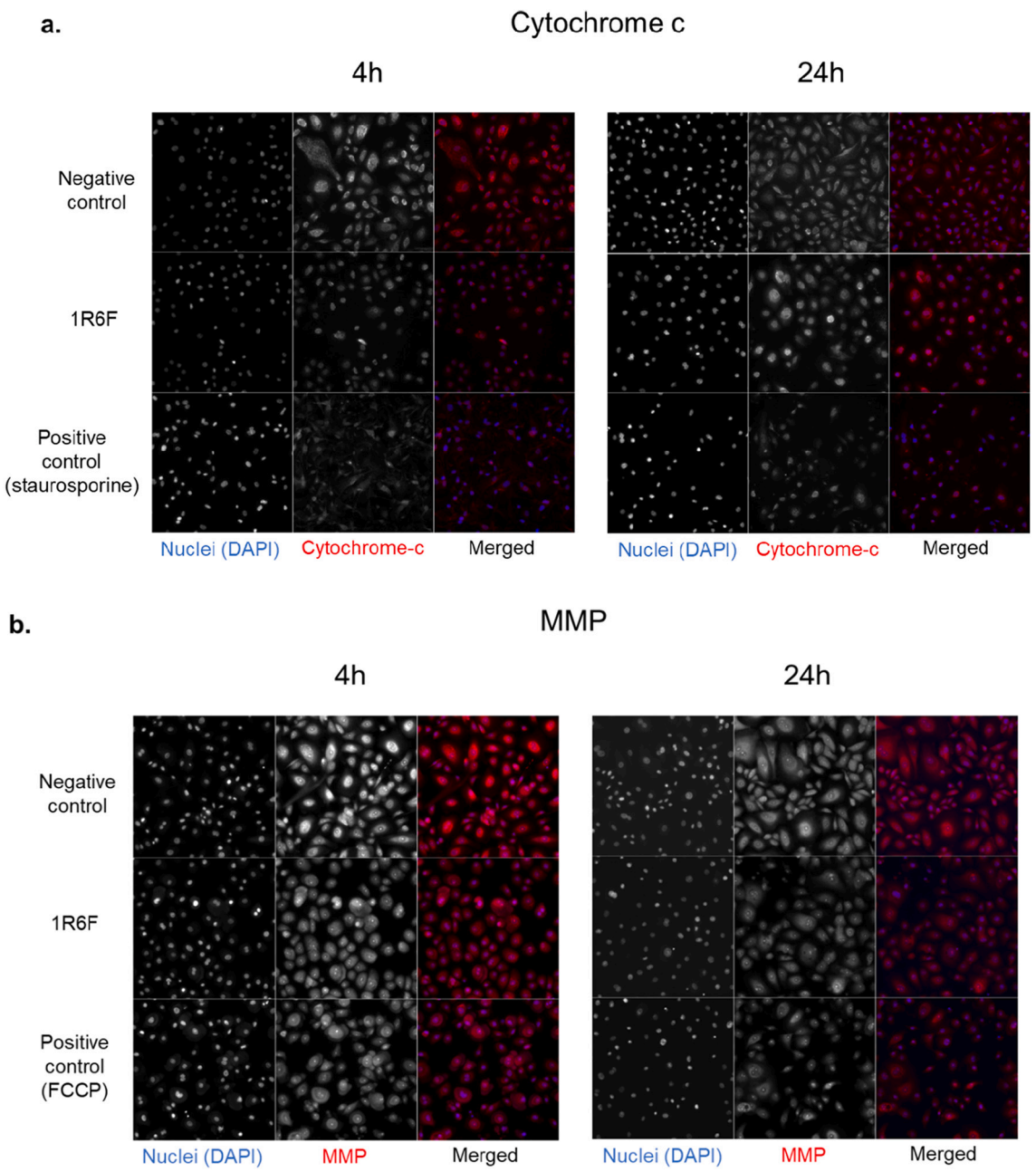

Fig. 7. Representative images of cells stained for the markers used in the HCS assay. Negative control: 10% bPBS; 1R6F concentration: 4% (selected due to this being the most potent test article); Positive control concentrations are detailed in Table S4.

significant, however, again, greatly reduced compared to the 1R6F response. This reinforces the reduced harm potential of the p-HTP products, however, as this is only one of many processes in the development of cardiovascular disease pathologies, investigation of the effects of the p-HTPs on further related endpoints, for example, inflammatory cell migration and markers (van der Toorn et al., 2015) may be useful.

4.3. HCS demonstrated sensitivity to the p-HTP and 1R6F samples, but responses were most substantial to 1R6F

In addition to the single endpoint assays used in this study, we utilised the mechanistically sensitive, multiple endpoint approach of HCS to gain further insight into the toxicological effects of the respective test articles. Cytotoxicity was observed with all three test articles at both 4 and 24 h, with the greatest measure in response to 1R6F and significant effects only seen at the highest two p-HTP concentrations tested. Some cytotoxicity with increasing dose was expected for all test articles, consistent with the results in the NRU and MN assays.

Cytochrome c has a role in mitochondria-driven apoptosis, through its release into the cytoplasm where it interacts with Apaf-1, leading to the formation of the apoptosome (Garrido et al., 2006). Here, a decrease in cytochrome *c* signal in the cytoplasm indicated this release from the mitochondria (resulting in less intense staining), and likely initiation of apoptotic events. This was the case for the 1R6F smoke bPBS after 4 h, and the effect increased in a dose-dependent manner, suggesting actions of the increasing concentrations of toxicants present. The actions of cytochrome *c* in apoptosis initiation do, however, have a threshold (Garrido et al., 2006), and in the future it may be useful to mark apoptotic cells within the cell population at the later timepoint to assess

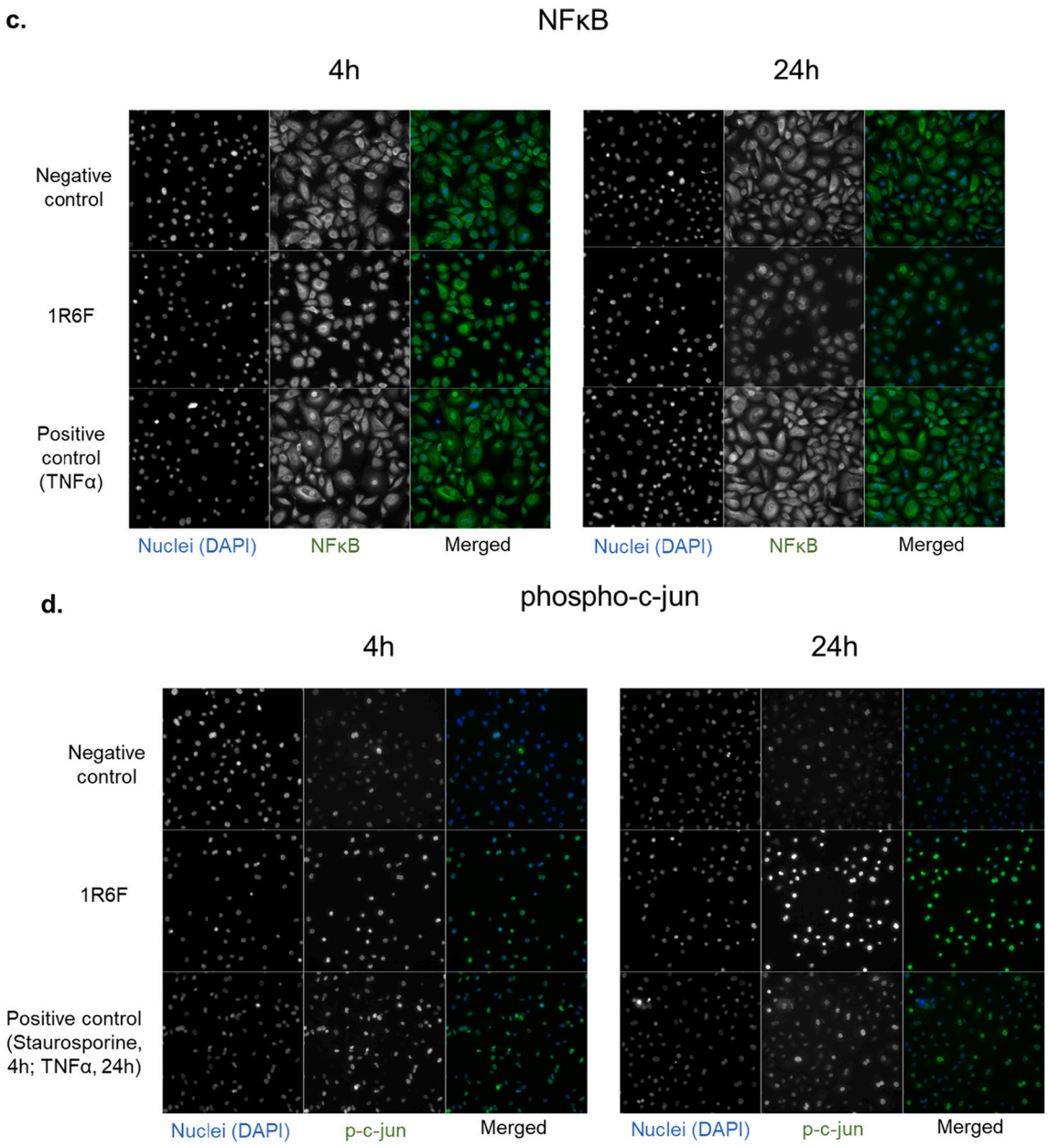

Fig. 7. (*continued*).

how much cell death is caused *via* this pathway. In contrast, following 24 h, at the higher 1R6F smoke bPBS test concentrations, the cytochrome *c* signal increased, suggesting increased respiratory activity within the mitochondria of the surviving population of cells under an adaptive response to the exposures. Interestingly, our observations of differing directions of cytochrome *c* response to the cigarette sample at 4 and 24 h are consistent with those seen by Kogel et al. (2015). Release of cytochrome *c*, along with other pro-apoptotic proteins, is coupled with a decrease in MMP (Elmore, 2007), and the observation of decreasing MMP with dose following 24 h may be linked to cytochrome *c* release at 4 h, or may also signal respiratory stress in the mitochondria, in line with increased cytochrome *c* signal 24 h following 1R6F exposure (Garrido et al., 2006).

Analysis of GSH levels was carried out at the earlier timepoint of 2 h to reflect the observed immediate reaction of GSH with the applied substances, and as responses at the 4 and 24 h timepoints were not conclusive (data not shown). In the presence of the 1R6F bPBS, we observed a dose-dependent decrease in GSH signal, indicating the presence of oxidative stressors in this sample, in contrast to the p-HTP bPBS. Some chemicals present in cigarette smoke, for example, carbonyls, as trapped in the bPBS (Tables S3.1 and S3.3, Supplementary information), have been demonstrated to form irreversible conjugates with GSH, causing a decrease in observed levels (van der Toorn et al., 2015). However, a lack of response compared to negative control at 4 and 24 h may indicate the reversible oxidation of GSH to GSSG in the presence of oxidative stressors at the 2 h timepoint. Furthermore, although the methods applied here were able to capture a short term response (at 2 h) in terms of GSH depletion with the 1R6F bPBS, this perhaps highlights a limitation in the current method's sensitivity to detect the effects of oxidative stressors present at the later timepoints of 4 and 24 h, and therefore, further optimisation with this endpoint is needed. Future studies with this screening approach would benefit from the addition of further endpoints addressing the presence of oxidative stress to verify this important acute impact on exposed cells.

Oxidative stress is one of many stimuli of the NfκB response. Its translocation to the nucleus is also associated with the presence of

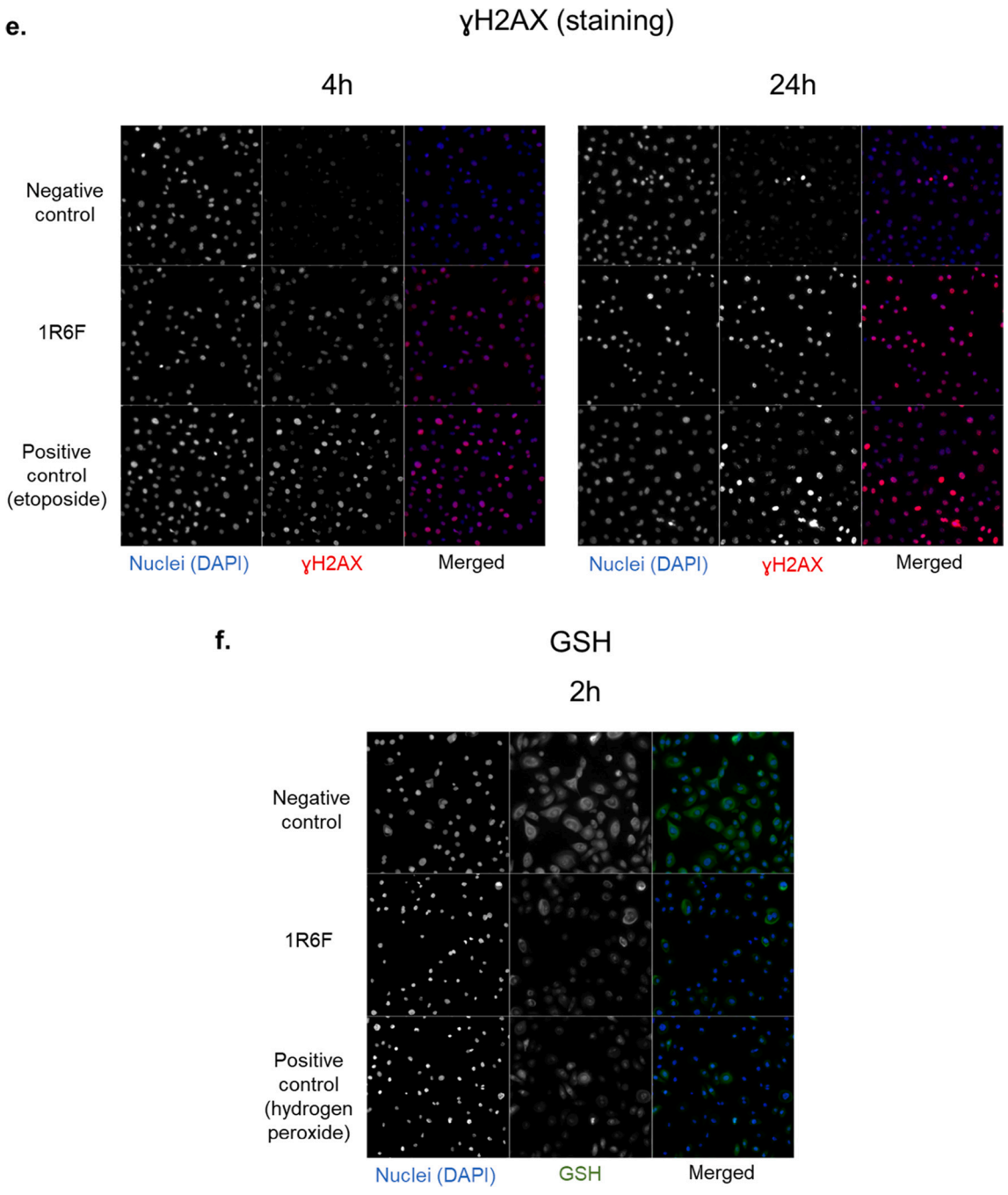

Fig. 7. (*continued*).

toxins, pro-inflammatory cytokines and cellular death signalling (Trask Jr., 2012). As chemical analyses confirmed trapping of smoke/ aerosol carbonyl constituents in the bPBS, the observation of NfκB activity at 4 and 24 h to all test articles was unsurprising. However, in correlation with the greater analyte levels in the 1R6F smoke bPBS compared to the p-HTP aerosol bPBS, the lesser extent of the p-HTP NfκB responses are understandable. These NfκB responses also confirm the sensitivity of the HCS approach.

Phosphorylation of c-jun is implicated in a number of cell stress related responses, including p53 related cell cycle and apoptosis regulation (Dreij et al., 2010). Here, we used the phosphorylation of c-jun as a general indicator of cell stress, and although there was some increased signal observed at 4 h, following exposure to higher p-HTP aerosol bPBS concentrations, this response was absent at 24 h. This indicates that the cell populations treated with p-HTP aerosol bPBS were able to adapt to the stress inducers present within the 24 h period. The 1R6F smoke bPBS exposures, however, resulted in even greater increases in phospho-c-jun signals with increasing dose, again consistent with the greater delivery of chemical stressors with this test article. However, at the top 1R6F test concentration, following 24 h, there was a decrease in signal, perhaps indicating an adaptive response in surviving cells. There also appeared to be a threshold for phosphorylation of c-jun in the presence of the 1R6F sample at a nicotine-scaled concentration of around 5 μg/ml.

The final endpoint tested with HCS was the phosphorylation of H2AX. Localised at the site of DNA double strand breaks (Garcia-Canton et al., 2014; Motoyama et al., 2018), γH2AX signal intensity can be correlated with the numbers of these DNA lesions following exposure. There were large increases in signal following both 4 and 24 h 1R6F

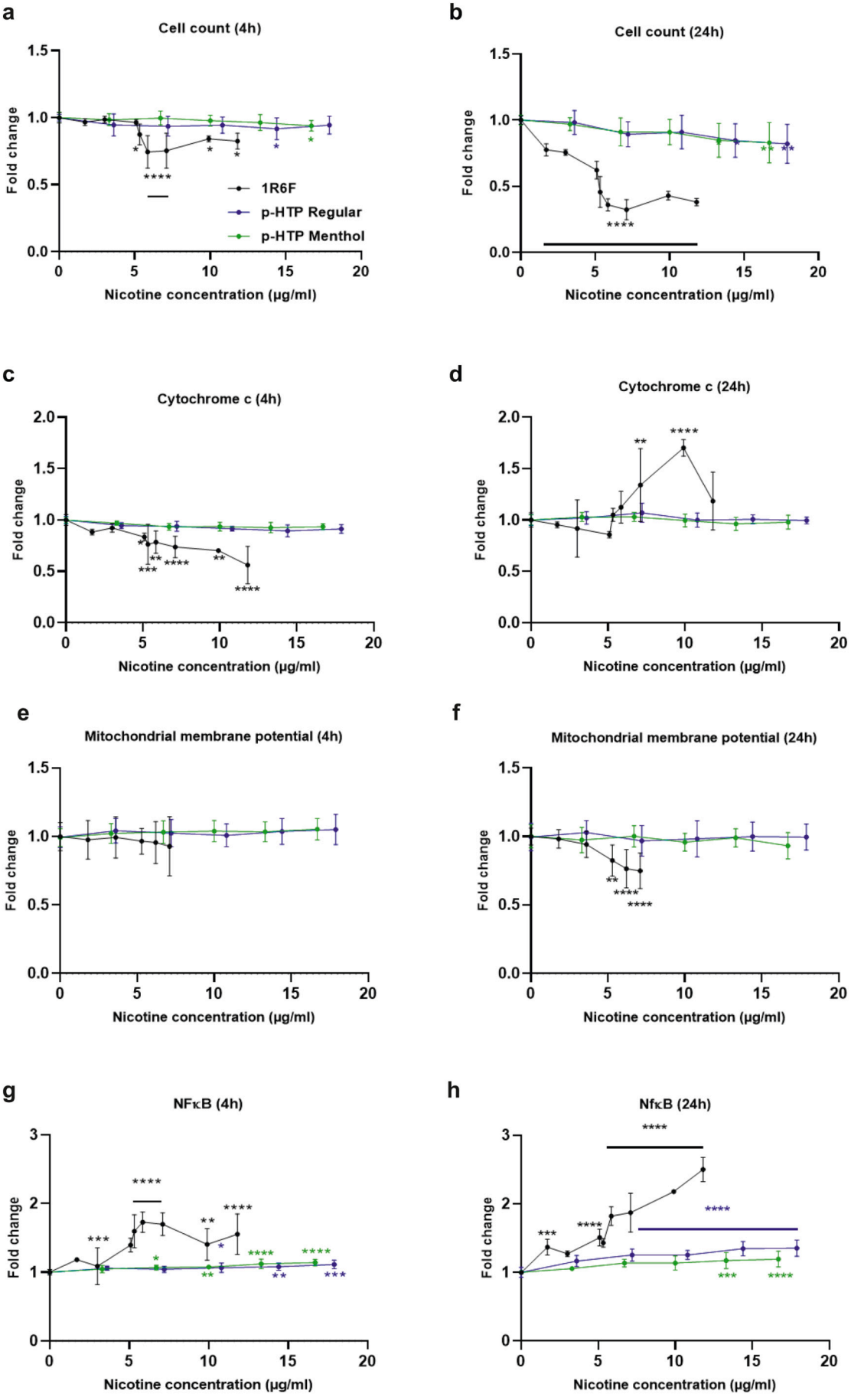
a
Cell count (4h)
Fold change
Nicotine concentration (µg/ml)
1R6F
p-HTP Regular
p-HTP Menthol
b
Cell count (24h)
Fold change
Nicotine concentration (µg/ml)
c
Cytochrome c (4h)
Fold change
Nicotine concentration (µg/ml)
d
Cytochrome c (24h)
Fold change
Nicotine concentration (µg/ml)
e
Mitochondrial membrane potential (4h)
Fold change
Nicotine concentration (µg/ml)
f
Mitochondrial membrane potential (24h)
Fold change
Nicotine concentration (µg/ml)
g
NFκB (4h)
Fold change
Nicotine concentration (µg/ml)
h
NfκB (24h)
Fold change
Nicotine concentration (µg/ml)

Fig. 8. Fold changes in seven high content screening endpoints measured following treatment of NHBE cells with PBS bubbled (bPBS) 1R6F Reference Cigarette smoke, p-HTP Menthol aerosol or p-HTP Regular aerosol for the indicated timeframes. Values are expressed as fold changes compared to the respective negative control signals and data is plotted on a nicotine concentration delivered to the cell culture medium in bPBS basis. Error bars represent standard deviation from the mean (SD); $n = 3$ (x3 technical replicates each). Significant responses in an ANOVA with Dunnett's post-hoc test are denoted by asterisks: $^{*}p < 0.05$, $^{**}p < 0.01$, $^{***}p < 0.001$, $^{****}p < 0.0001$. Puffs/ml concentrations corresponding to the plotted nicotine concentrations can be found in the Supplementary information (Table S3.3).

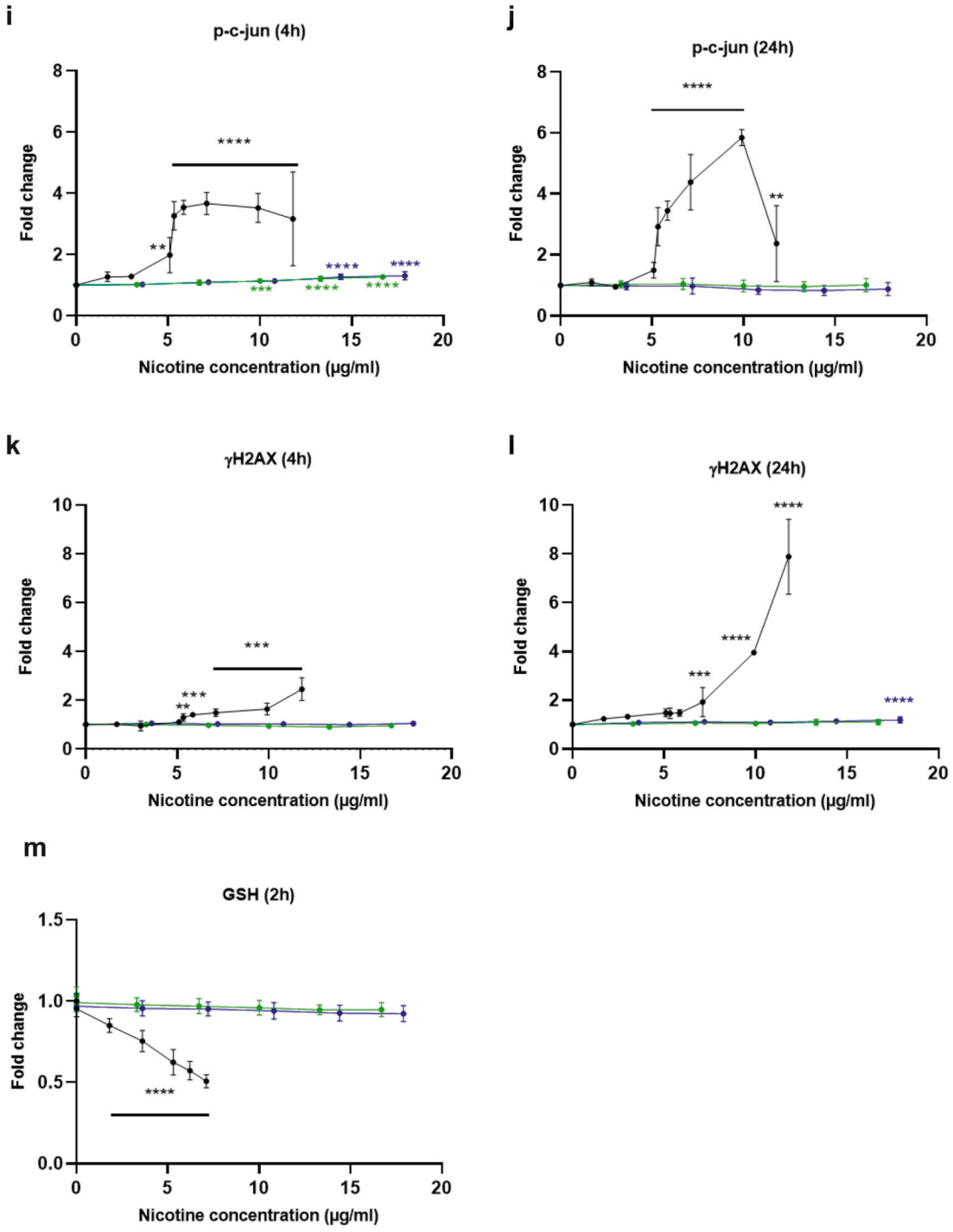

Fig. 8. (*continued*).

smoke bPBS exposures, and these responses were much greater at the 24 h timepoint. The particular occurrence of pan-nuclear staining patterns at the 24 h timepoint indicates the activation of multiple pathways leading to an overall phosphorylation of H2AX over the 24 h time period, analogous with mechanisms described elsewhere (Solier and Pommier, 2009). This signals the occurrence of some secondary DNA damage, perhaps from the presence of oxidative species associated with the cellular stress response over the 24 h period. There was also a small, but significant, signal at the top test concentration of the p-HTP Regular aerosol bPBS, again indicating, but to a much lesser extent, some secondary DNA damage here. On comparison of the DNA damage observed in the HCS analyses and MN assay, p-HTP-induced DNA damage was more evident in the MN assay. This may be attributed to the use of whole aerosol for exposures in the MN assay, including exposure to

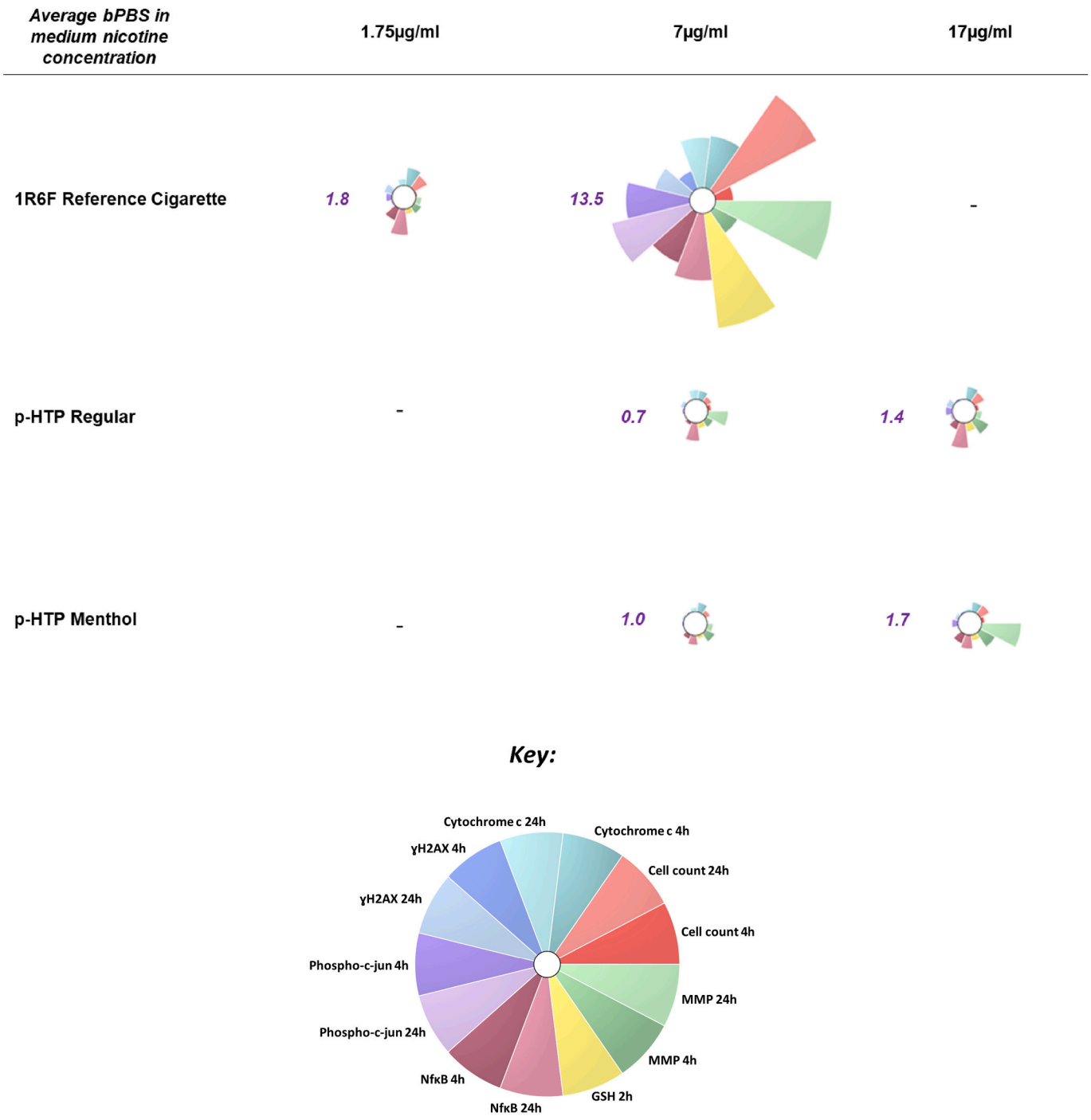

Fig. 9. ToxPi visual plots of HCS outputs at a low nicotine concentration (1.75 µg/ml = 0.019puffs/ml for 1R6F), at an equivalent (7 ± 0.3 µg/ml = approx. 0.075puffs/ml for 1R6F and 0.18puffs/ml for the p-HTPs) and a high nicotine concentration (17 ± 0.9 µg/ml = 0.45puffs/ml for the p-HTPs). Relative potency scores generated from the data of each plot are also detailed in purple italics. Plotted fold changes in responses (compared to respective background levels (set to 1-fold)) are scaled according to the maximum values observed for each endpoint (over both 4 and 24 h) across all doses and samples tested (detailed in Figs. 8 and 9; note, highest fold responses (in either direction) were always induced by 1R6F). The key plot represents these maximum values and indicates which slices correspond to which endpoint and timepoint. (For interpretation of the references to colour in this figure legend, the reader is referred to the web version of this article.)

hydrophobic fractions of the aerosol which may not be soluble within the aqueous bPBS, or indeed cell culture medium (Smart and Phillips, 2021). However, as the HCS analysis was carried out in human cells (NHBEs) up to a timepoint of 24 h only, without an indication of MN formation, and the MN assay in rodent (V79) cells, it is difficult to draw direct comparisons between the results.

Nicotine concentrations are often used to draw comparisons between the effects of different products (Czekala et al., 2019), therefore the HCS results were expressed on a nicotine concentration scale. When considering the HCS results as a whole for each test article, and at comparable nicotine concentrations, it was possible to gain an idea of the relative potencies of the test articles. The ToxPi plots acted as a tool for visual comparison of responses at selected exposures, and the numerical inputs were used to score each test article on their overall HCS responses. At a comparable nicotine concentration in the cell culture medium of 7 µg/ml, 1R6F scored 13.5 compared to 0.7 for p-HTP Menthol and 1.0 for p-

HTP Regular. Only when compared at a 1R6F nicotine concentration 10 times lower than those delivered by the p-HTPs, did the products have similar potencies. This output may be able to provide a means of ranking different products for their placement on a product risk spectrum and their harm reduction potential. Although the test articles were compared on a nicotine concentration basis, it is unlikely that nicotine was driving any of the observed responses in the HCS analyses. Testing of e-liquids containing nicotine in a range of HCS endpoints, some overlapping with those used here (GSH, cytochrome *c*, phospho-c-jun), by Iskandar et al. (2018), did not result in effects in NHBE cells at nicotine scaled concentrations well in excess of those applied here.

Future HCS could incorporate further endpoints to indicate further cell stress responses, for example, cell cycling changes, mitochondrial mass (content), cell death pathways and inflammatory markers related to specific disease endpoints and in disease-specific cell types, or even the analysis of 3D cultures (Taylor et al., 2018; Iskandar et al., 2018). We applied exposures within bPBS, to the aqueous soluble fractions of smoke/aerosol, however, comparison of the responses observed here to those to whole smoke/aerosol may provide further mechanistic insights. This part of the study was also limited by the absence of ALI stimulation and exposure of the cells, which may increase the human relevance of the assay further.

The overall substantial reductions in toxicological responses in the *in vitro* tests used correspond to the substantial reductions in levels and numbers of toxicants measured in the aerosol compared to 1R6F smoke (Table S1), reinforcing the translation of reduced toxicant exposure to reduced toxicological effects proposed for HTPs (Hattori et al., 2020; Schaller et al., 2016; Dusautoir et al., 2021; Breheny et al., 2017; Jaunky et al., 2018; Kogel et al., 2015; Taylor et al., 2018; Wang et al., 2021; Scharf et al., 2021; Horinouchi and Miwa, 2021).

4.4. Evaluation of the study and future direction

This study used a combination of established *in vitro* toxicological assays to assess the effects of p-HTP variants compared to the 1R6F Reference Cigarette, combined with aerosol/smoke chemistry analysis. This multiple endpoint assessment extended upon the approach taken by Rudd et al. (2020) to include further disease-related markers, using the cardiovascular scratch wound assay and HCS to indicate mechanisms of cellular stress responses. However, whilst each individual endpoint adds to the weight of evidence that p-HTPs may offer a potentially reduced harm alternative to adult smokers, this framework would benefit from the addition of other disease-related endpoints and cell models to substantiate this further. These could include 3D lung models exposed to whole aerosol, and further cardiovascular disease-related assessments. In addition to this, analyses at the transcriptomic, proteomic or metabolomic level could provide indications of additional pathways involved in the cellular responses to the p-HTP aerosols (Iskandar et al., 2018). Application of quantitative *in vitro* to *in vivo* extrapolation (QVIVE) approaches also enable linking of *in vitro* effective exposure levels and the human exposure scenario. A separate study has been carried out to model blood nicotine concentrations and an associated minimum effective concentration (MEC) for the p-c-jun endpoint (derived from an *in vitro* study; data not shown). The predicted MEC of deposited nicotine in the respiratory tract, was 125.6 μg nicotine, which equated to a predicted steady state blood nicotine concentration of 94.31 ng/ml. This blood nicotine concentration is substantially higher than even a maximum concentration (C_{max}) generally observed for the heated tobacco category (Phillips-Waller et al., 2021; Hardie et al., 2022). The substantial reductions in toxicants compared to combustible cigarette smoke, combined with the unrealistically high level of relative blood nicotine associated with the MEC for the HTP aerosol constituent mixture, adds further evidence for the THR potential for HTPs, however, it must be acknowledged that this is based on one toxicological endpoint and application of the multiple endpoint approach, such as that used in this study, would potentially provide more informative outcomes. This would also need to be combined with consideration of the pharmacokinetics of all constituents of the aerosol mixture. However, this information may still be useful in the design of future studies which may include the assessment of toxicological outcomes in exposure-relevant (cell) models. For example, Li et al. (2021) recently predicted that the deposition of heated tobacco and e-cigarette products' particles had higher deposition potential in all regions of the lung compared to conventional cigarette (under the model standard puffing parameter) and this could be influenced by different puffing parameters; such information could inform on how relative *in vitro* exposures of different products should be applied, and to which cell models.

When considering a combination of all endpoints, the p-HTPs exhibited measurable toxicological effects, particularly at the higher test doses. These products, as mentioned earlier, are placed on a risk continuum along with other NGPs such as oral tobacco-free nicotine pouches and e-cigarettes. However, it must still be highlighted that HTPs do offer adult smokers a sensory experience and satisfaction closer to combustible cigarette smoking, but in a significantly less harmful way than smoking, and so may have greater tobacco harm reduction potential over other products that sit further down the risk continuum, through potentially higher acceptance rates of HTPs by adult smokers (Roulet et al., 2019; Farsalinos et al., 2019). As HTPs provide adult smokers with this sensory satisfaction and delivery of desired levels of nicotine (Haziza et al., 2020), many adult smokers who do not find this with other tools such as EVP use, for example, they do not like the taste (Roulet et al., 2019), might find HTPs a more effective tool for off-ramping from combustible cigarettes and moving away from smoking. This is supported by the sustained use of HTPs following transitioning from combustible cigarette use in adult smokers (Roulet et al., 2019; Farsalinos et al., 2019).

As HTPs are a growing product category, there is no consensus yet on technical and testing standards, for example, user representative puffing regimes (as with ISO 20768 ISO (2018a) for e-cigarettes) and stick conditioning standards. Here, we conditioned sticks according to ISO 3402, as is applied in combustible cigarette testing. There is evidence that HTP sticks tested for aerosol emissions under various conditioning regimes does not result in compositional differences (Schaller et al., 2016), however, this needs to be confirmed for the p-HTPs used in this study. ISO 20778 was selected as this regime is considered to represent a maximal exposure and emissions scenario (Forster et al., 2018).

In terms of the smoke/ aerosols tested here, we applied exposures both in the whole and aqueous soluble forms. As mentioned previously, analysis confirmed trapping of constituents such as nicotine and carbonyls within the bPBS, but this is not representative of the whole smoke/ aerosol, and as such, induced perhaps lower effects than if other fractions of the smoke had been present. Smart and Phillips (2021) have previously highlighted the limitations of generating extracts from complex mixtures generated from NGPs for *in vitro* exposures. The constituents of aerosols/ smoke, such as those generated from the products used in this study, possess a wide range of chemical properties, for example, different aqueous solubilities and volatilities. These inherent chemical properties can influence not only how effectively different chemicals are trapped for addition to *in vitro* systems (Smart and Phillips, 2021), but also nominal exposure concentrations and relative bioavailability when applied *in vitro* (Groothuis et al., 2015). For example, in generating aqueous extracts, trapping of hydrophobic compounds may be inefficient, volatiles may be lost in certain extraction processes, and use of solvents such as DMSO are common (Smart and Phillips, 2021). Furthermore, when samples are added to the cell culture environment, preferential binding of hydrophobic compounds to the various constituents (plate plastic, serum, cell lipid layers, *etc.*), effects of solvents, like DMSO, and further volatile losses which may occur during exposure, may limit chemical bioavailability (Chapman et al., 2020). Therefore, these factors could potentially result in a reduction in effects compared to those that may be seen with whole smoke/ aerosol exposures, which would contain a greater number of chemical

constituents than the various forms of extracts, and can be delivered fresh following generation. However, our approach of applying whole smoke/ aerosol at the ALI in the MN and NRU assays using the custom built SAEIVS, and in the Ames assay using fresh smoke/ aerosol generated by the Vitrocell VC 10 S-Type smoking machine passed through impingers, allows better representation of all chemical fractions during exposure, and therefore is an invaluable approach for inhalable NGP assessment. With whole aerosol/ smoke exposure, particularly the ALI exposures using the SAEIVS, the cells are exposed to as many chemical constituents generated from the products as possible, which is potentially more consumer relevant. Whilst the loss of volatile compounds, and also aerosol/ smoke ageing, may be a risk during whole aerosol/ smoke exposures, the SAEIVS delivers smoke in under 10s, to mitigate this. It is also important to acknowledge that for the fractions of applied chemicals that are bioavailable and taken up by the cells, the variant metabolic capabilities of different cell types/ lines may also influence the effects of pro-toxicants (Garcia-Canton et al., 2013).

The cell models selected in this study provided a useful tool for the initial screening of the relative effects of the test articles. However, future work would expand upon this to further refine the assessment framework. This would include the application of HCS in further donors to elucidate the role of donor variability on the toxicological outcomes observed. Furthermore, whilst the HCS assay was carried out in undifferentiated NHBE cells for this early screening approach, further characterisation of the cells in a differentiated state may further increase the relevance of toxicological outcomes to exposures applied. In addition, the cell models used could be refined further to increase human relevance of the outcomes assessed. Particularly, V79 is a rodent-derived cell line, and in the future it may be more informative to optimise the ALI exposure using human-derived cells for the micronucleus assay to more closely model the DNA damage response in humans. To further characterise the effects of the test articles, it would also be interesting to expand the number of endpoints screened, for example, within the HCS assay, or in other models such as 3D lung and cardiovascular models, to assess further endpoints associated with smoking-related disease development and progression. To this end, assessment of inflammatory and immune responses would be of interest for exposure with the test articles in this study.

Finally, to further characterise the different toxicological mechanisms of the p-HTP aerosols and (1R6F) cigarette smoke, the use of positive control compounds of known public health interest, and associated with cigarette smoke, for example, cadmium or B[*a*]P, would be useful. For example, if a signature for responses across the HCS endpoint for such control compounds could be characterised and matched against those for the test article to potentially define the contribution of these chemicals to the responses observed, or highlight the absence, or reduction of these responses in the case of HTP.

4.5. Conclusions

HTPs form a growing category of potentially reduced harm nicotine delivery for adult smokers who would otherwise continue smoking. Overall, this study has applied aerosol/ smoke chemical compositional analysis, combined with a multiple endpoint *in vitro* toxicological assessment framework, to compare p-HTP samples with the 1R6F Reference Cigarette. This is not only the first study of this kind using this type of p-HTP but is also the first published application of our multiple endpoint weight of evidence testing approach, covering a number of smoking induced disease-related toxicological processes, which can also be used to assess further NGPs. This study has highlighted substantial reductions in HPHC levels within the p-HTP aerosols compared to 1R6F smoke, reflected by reductions in the measured *in vitro* toxicological responses, and has provided mechanistic insights into the biological effects of the p-HTPs. Our findings add to the growing weight of evidence behind the role the HTP category, including the p-HTPs tested, may play in THR by providing adult smokers with an acceptable and satisfying reduced harm mode of nicotine delivery compared to combustible cigarettes and gives confidence to move into clinical assessment with adult smokers.

Funding statement

This work was funded by Imperial Brands PLC.

Declaration of Competing Interest

The authors declare the following financial interests/personal relationships which may be considered as potential competing interests:

Fiona Chapman reports a relationship with Imperial Brands plc that includes: employment. Edgar Trelles Sticken reports a relationship with Imperial Brands plc that includes: employment. Roman Wieczorek reports a relationship with Imperial Brands plc that includes: employment. Sarah Jean Pour reports a relationship with Imperial Brands plc that includes: employment. Ole Dethloff reports a relationship with Imperial Brands plc that includes: employment. Jessica Budde reports a relationship with Imperial Brands plc that includes: employment. Kathryn Rudd reports a relationship with Imperial Brands plc that includes: employment. Elizabeth Mason reports a relationship with Imperial Brands plc that includes: employment. Lukasz Czekala reports a relationship with Imperial Brands plc that includes: employment. Fan Yu reports a relationship with Imperial Brands plc that includes: employment. Liam Simms reports a relationship with Imperial Brands plc that includes: employment. Thomas Nahde reports a relationship with Imperial Brands plc that includes: employment. Grant O'Connell reports a relationship with Imperial Brands plc that includes: employment. Matthew Stevenson reports a relationship with Imperial Brands plc that includes: employment.

Data availability

Data will be made available on request.

Acknowledgements

The authors would like to thank the Imperial Brands internal Reading Committee for their critical review of the manuscript. This work was funded by Imperial Brands plc.

Appendix A. Supplementary data

Supplementary data to this article can be found online at https://doi.org/10.1016/j.tiv.2022.105510.

References

Akiyama, Y., Sherwood, N., 2021. Systematic review of biomarker findings from clinical studies of electronic cigarettes and heated tobacco products. Toxicol. Rep. 8, 282–294. https://doi.org/10.1016/j.toxrep.2021.01.014.

Bekki, K., Inaba, Y., Uchiyama, S., Kunugita, N., 2017. Comparison of chemicals in mainstream smoke in heat-not-burn tobacco and combustion cigarettes. J. UOEH 39 (3), 201–207. https://doi.org/10.7888/juoeh.39.201.

Belcastro, V., Cano, S., Marescotti, D., Acali, S., Poussin, C., Gonzalez-Suarez, I., Martin, F., Bonjour, F., Ivanov, N., Peitsch, M., Hoeng, J., 2019. Gladiatox: global assessment of dose-indicator in toxicology. Bioinformatics 35 (20), 4190–4192. https://doi.org/10.1093/bioinformatics/btz187.

Benowitz, N., Hukkanen, J., Jacob, P., 2009. Nicotine chemistry, metabolism, kinetics and biomarkers. Handb. Exp. Pharmacol. 192, 29–60. https://doi.org/10.1007/978-3-540-69248-5_2.

Bentley, M., Almstetter, M., Arndt, D., Knorr, A., Martin, E., Pospisil, P., Maeder, S., 2020. Comprehensive chemical characterization of the aerosol generated by a heated tobacco product by untargeted screening. Anal. Bioanal. Chem. 412 (11), 2675–2685. https://doi.org/10.1007/s00216-020-02502-1.

Bishop, E., Breheny, D., Hewitt, K., Taylor, M., Jaunky, T., Camacho, O., Thorne, D., Gaça, M., 2020. Evaluation of a high-throughput in vitro endothelial cell migration assay for the assessment of nicotine and tobacco delivery products. Toxicol. Lett. https://doi.org/10.1016/j.toxlet.2020.07.011.

Breheny, D., Adamson, J., Azzopardi, D., Baxter, A., Bishop, E., Carr, T., Crooks, I., Hewitt, K., Jaunky, T., Larard, S., Lowe, F., Oke, O., Taylor, M., Santopietro, S., Thorne, D., Zainuddin, B., Gaça, M., Liu, C., Murphy, J., Proctor, C., 2017. A novel hybrid tobacco product that delivers a tobacco flavour note with vapour aerosol (part 2): in vitro biological assessment and comparison with different tobacco-heating products. Food Chem. Toxicol. 106 (Pt A), 533–546. https://doi.org/10.1016/j.fct.2017.05.023.

Brossard, P., Weitkunat, R., Poux, V., Lama, N., Haziza, C., Picavet, P., Baker, G., Lüdicke, F., 2017. Nicotine pharmacokinetic profiles of the tobacco heating system 2.2, cigarettes and nicotine gum in Japanese smokers. Regul. Toxicol. Pharmacol. 89, 193–199. https://doi.org/10.1016/j.yrtph.2017.07.032.

Buratto, R., Correia, D., Parel, M., Crenna, M., Bilger, M., Debrick, A., 2018. Determination of eight carbonyl compounds in aerosols trapped in phosphate buffer saline solutions to support in vitro assessment studies. Talanta 184, 42–49. https://doi.org/10.1016/j.talanta.2018.02.048.

Burns, D., Dybing, E., Gray, N., Hecht, S., Anderson, C., Sanner, T., O'Connor, R., Djordjevic, M., Dresler, C., Hainaut, P., Jarvis, M., Opperhuizen, A., Straif, K., 2008. Mandated lowering of toxicants in cigarette smoke: a description of the world health organization tobreg proposal. Tob. Control. 17, 132–141. https://doi.org/10.1136/tc.2007.024158.

Chapman, F., Sparham, C., Hastie, C., Sanders, D., van Egmond, R., Chapman, K., Doak, S., Scott, A., Jenkins, G., 2020. Comparison of passive-dosed and solvent spiked exposures of procarcinogen, benzo[a]pyrene, to human lymphoblastoid cell line, MCL-5. Toxicol. in Vitro 67, 104905. https://doi.org/10.1016/j.tiv.2020.104905.

CORESTA Heated Tobacco Products Task Force, 2020. Technical Report: Heated Tobacco Products (HTPs): Standardized Terminology and Recommendations for the Generation and Collection of Emissions. Ref. HTP-259-CTR. https://www.coresta.org/sites/default/files/technical_documents/main/HTP-259-CTR_Std-Terminology-Recommendations-HTP-Emissions_July2020.pdf.

Cozzani, V., Barontini, F., McGrath, T., Mahler, B., Nordlund, M., Smith, M., Schaller, J., Zuber, G., 2020. An experimental investigation into the operation of an electrically heated tobacco system. Thermochim. Acta 684, 178475. https://doi.org/10.1016/j.tca.2019.178475.

Crooks, I., Neilson, L., Scott, K., Reynolds, L., Oke, T., Forster, M., Meredith, C., McAdam, K., Proctor, C., 2018. Evaluation of flavourings potentially used in a heated tobacco product: chemical analysis, in vitro mutagenicity, genotoxicity, cytotoxicity and in vitro tumour promoting activity. Food Chem. Toxicol. 118, 940–952. https://doi.org/10.1016/j.fct.2018.05.058.

Czekala, L., Simms, L., Stevenson, M., Trelles Sticken, E., Walker, P., Walele, T., 2019. High content screening in NHBE cells shows significantly reduced biological activity of flavoured e-liquids, when compared to cigarette smoke condensate. Toxicol. in Vitro 58, 86–96. https://doi.org/10.1016/j.tiv.2019.03.018.

Czekala, L., Chapman, F., Simms, L., Rudd, K., Trelles Sticken, E., Wieczorek, R., Bode, L., Pani, J., Moelijker, N., Derr, R., Brandsma, I., Hendriks, G., Stevenson, M., Walele, T., 2021. The in vitro toxtracker and aneugen clastogen evaluation extension assay as a tool in the assessment of relative genotoxic potential of e-liquids and their aerosols. Mutagenesis. https://doi.org/10.1093/mutage/geaa033.

Davis, B., To, V., Talbot, P., 2019. Comparison of cytotoxicity of IQOS aerosols to smoke from Marlboro red and 3R4F reference cigarettes. Toxicol. in Vitro 61, 104652. https://doi.org/10.1016/j.tiv.2019.104652.

Dillon, D., Combes, R., Zeiger, E., 1998. The effectiveness of Salmonella strains TA100, TA102 and TA104 for detecting mutagenicity of some aldehydes and peroxides. Mutagenesis 13 (1), 19–26. https://doi.org/10.1093/mutage/13.1.19.

Dreij, K., Rhrissorrakrai, K., Gunsalus, K., Geacintov, N., Scicchitano, D., 2010. Benzo[a]pyrene diol epoxide stimulates an inflammatory response in normal human lung fibroblasts through a p53 and JNK mediated pathway. Carcinogenesis 31 (6), 1149–1157. https://doi.org/10.1093/carcin/bgq073.

Dusautoir, R., Zarcone, G., Verriele, M., Garçon, G., Fronval, I., Beauval, N., Allorge, D., Riffault, V., Locoge, N., Lo-Guidice, J., Anthérieu, S., 2021. Comparison of the chemical composition of aerosols from heated tobacco products, electronic cigarettes and tobacco cigarettes and their toxic impacts on the human bronchial epithelial BEAS-2B cells. J. Hazard. Mater. 401, 123417 https://doi.org/10.1016/j.jhazmat.2020.123417.

Eaton, D., Jakaj, B., Forster, M., Nicol, J., Mavropoulou, E., Scott, K., Liu, C., McAdam, K., Murphy, J., Proctor, C., 2018. Assessment of tobacco heating product THP1.0. Part 2: product design, operation and thermophysical characterisation. Regul. Toxicol. Pharmacol. 93, 4–13. https://doi.org/10.1016/j.yrtph.2017.09.009.

Elmore, S., 2007. Apoptosis: a review of programmed cell death. Toxicol. Pathol. 35 (4), 495–516.

Farsalinos, K., Yannovits, N., Sarri, T., Voudris, V., Poulas, K., 2017. Nicotine delivery to the aerosol of a heat-not-burn tobacco product: comparison with a tobacco cigarette and E-cigarettes. Nicotine Tob. Res. 20 (8), 1004–1009. https://doi.org/10.1093/ntr/ntx138.

Farsalinos, K., Diamantopoulou, E., Panagiotopoulou, E., Barbouni, A., 2019. Patterns of use, past smoking status, and biochemically verified current smoking status of heated tobacco product (IQOS) shops customers: preliminary results. CHEST 155 (6), A387. https://doi.org/10.1016/j.chest.2019.04.089.

Fearon, I., Acheampong, D., Bishop, E., 2012. Modification of smoke toxicant yields alters the effects of cigarette smoke extracts on endothelial migration: an in vitro study using a cardiovascular disease model. Int. J. Toxicol. 31 (6), 572–583. https://doi.org/10.1177/1091581812461810.

Fearon, I.M., Gaça, M., Nordskog, B., 2013. In vitro models for assessing the potential cardiovascular disease risk associated with cigarette smoking. Toxicol. in Vitro 27 (1), 513–522. https://doi.org/10.1016/j.tiv.2012.08.018.

Fenech, M., 1993. The cytokinesis-block micronucleus technique: a detailed description of the method and its application to genotoxicity studies in human populations. Mutat. Res. 285 (1), 35–44. https://doi.org/10.1016/0027-5107(93)90049-l.

Forster, M., Fiebelkorn, S., Yurteri, C., Mariner, D., Liu, C., Wright, C., McAdam, K., Murphy, J., Proctor, C., 2018. Assessment of novel tobacco heating product THP1.0. Part 3: comprehensive chemical characterisation of harmful and potentially harmful aerosol emissions. Regul. Toxicol. Pharmacol. 93, 14–33. https://doi.org/10.1016/j.yrtph.2017.10.006.

Fowler, P., Smith, K., Young, J., Jeffrey, L., Kirkland, D., Pfuhler, S., Carmichael, P., 2012. Reduction of misleading ("false") positive results in mammalian cell genotoxicity assays. I. Choice of cell type. Mutat. Res. 742 (1–2), 11–25. https://doi.org/10.1016/j.mrgentox.2011.10.014.

Garcia-Canton, C., Minet, E., Anadon, A., Meredith, C., 2013. Metabolic characterization of cell systems used in in vitro toxicology testing: lung cell system BEAS-2B as a working example. Toxicol. in Vitro 27 (6), 1719–1727.

Garcia-Canton, C., Errington, G., Anadon, A., Meredith, C., 2014. Characterisation of an aerosol exposure system to evaluate the genotoxicity of whole mainstream cigarette smoke using the in vitro γH2AX assay by high content screening. BMC Pharmacol. Toxicol. 15, 41. https://doi.org/10.1186/2050-6511-15-41.

Garrido, C, Galluzzi, L, Brunet, M, Puig, PE, Didelot, C, Kroemer, G, 2006 Sep. Mechanisms of cytochrome c release from mitochondria. Cell Death Differ 13 (9), 1423–1433. https://doi.org/10.1038/sj.cdd.4401950. Epub 2006 May 5. PMID: 16676004.

Gee, J., Prasad, K., Slayford, S., Gray, A., Nother, K., Cunningham, A., Mavropoulou, E., Proctor, C., 2018. Assessment of tobacco heating product THP1.0. Part 8: study to determine puffing topography, mouth level exposure and consumption among Japanese users. Regul. Toxicol. Pharmacol. 93, 84–91.

Godec, T.L., Crooks, I., Scott, K., Meredith, C., 2019. In vitro mutagenicity of gas-vapour phase extracts from flavoured and unflavoured heated tobacco products. Toxicol. Rep. 6, 1155–1163. https://doi.org/10.1016/j.toxrep.2019.10.007.

Gonzalez-Suarez, I., Martin, F., Marescotti, D., Guedj, E., Acali, S., Johne, S., Dulize, R., Baumer, K., Peric, D., Goedertier, D., Frentzel, S., Ivanov, N., Mathis, C., Hoeng, J., Peitsch, M., 2016. In vitro systems toxicology assessment of a candidate modified risk tobacco product shows reduced toxicity compared to that of a conventional cigarette. Chem. Res. Toxicol. 29 (1), 3–18. https://doi.org/10.1021/acs.chemrestox.5b00321.

Groothuis, F., Heringa, M., Nicol, B., Hermens, J., Blaauboer, B., Kramer, N., 2015. Dose metric considerations in in vitro assays to improve quantitative in vitro-in vivo dose extrapolations. Toxicology 332, 30–40. https://doi.org/10.1016/j.tox.2013.08.012.

Hardie, G., Gale, N., McEwan, M., Oscar, S., Ziviani, L., Proctor, C., Murphy, J., 2022. An abuse liability assessment of the glo tobacco heating product in comparison to combustible cigarettes and nicotine replacement therapy. Sci. Rep. 12 (1), 14701.

Hattori, N., Nakagawa, T., Yoneda, M., Nakagawa, K., Hayashida, H., Ito., T., 2020. Cigarette smoke, but not novel tobacco vapor products, causes epigenetic disruption and cell apoptosis. Biochem. Biophys. Rep. 24, 100865 https://doi.org/10.1016/j.bbrep.2020.100865.

Haziza, C., de La Bourdonnaye, G., Donelli, A., Poux, V., Skiada, D., Weitkunat, R., Baker, G., Picavet, P., Lüdicke, F., 2020. Reduction in exposure to selected harmful and potentially harmful constituents approaching those observed upon smoking abstinence in smokers switching to the menthol tobacco heating system 2.2 for 3 months (part 1). Nicotine Tob. Res. 22 (4), 539–548. https://doi.org/10.1093/ntr/ntz013.

Horinouchi, T., Miwa, S., 2021. Comparison of cytotoxicity of cigarette smoke extract derived from heat-not-burn and combustion cigarettes in human vascular endothelial cells. J. Pharmacol. Sci. 147 (3), 223–233. https://doi.org/10.1016/j.jphs.2021.07.005.

Hüttemann, M., Pecina, P., Rainbolt, M., Sanderson, T., Kagan, V., Samavati, L., Doan, J., Lee, I., 2011. The multiple functions of cytochrome c and their regulation in life and death decisions of the mammalian cell: from respiration to apoptosis. Mitochondrion 11 (3), 369–381. https://doi.org/10.1016/j.mito.2011.01.010.

International Agency for Research on Cancer, 2012. Personal Habits and Indoor Combustions. A Review of Human Carcinogens: IARC Monographs on the Evaluation of Carcinogenic Risks to Humans. Volume 100E. https://monographs.iarc.fr/wp-content/uploads/2018/06/mono100E.pdf (Last accessed 13-02-2021).

Iskandar, A., Martin, F., Leroy, P., Schlage, W., Mathis, C., Titz, B., Kondylis, A., Schneider, T., Vuillaume, G., Sewer, A., Guedj, E., Trivedi, K., Elamin, A., Frentzel, S., Ivanov, N., Peitsch, M., Hoeng, J., 2018. Comparative biological impacts of an aerosol from carbon-heated tobacco and smoke from cigarettes on human respiratory epithelial cultures: a systems toxicology assessment. Food Chem. Toxicol. 115, 109–126. https://doi.org/10.1016/j.fct.2018.02.063.

ISO, 1999. ISO 3402:1999: tobacco and tobacco products - atmosphere for conditioning and testing. ICS 65 (65), 160. https://www.iso.org/standard/28324.html.

ISO, 2012. Routine analytical cigarette-smoking machine — definitions and standard conditions. ICS 65 (65), 160. https://www.iso.org/standard/60404.html.

ISO, 2018a. ISO 20768:2018 - vapour products - routine analytical vaping machine - definitions and standard conditions. ICS 65 (65), 160. https://www.iso.org/standard/69019.html.

ISO, 2018b. ISO 20778:2018 - cigarettes - routine analytical cigarette smoking machine - definitions and standard conditions with an intense smoking regime. ICS 65 (65), 160. https://www.iso.org/standard/69065.html.

Jaccard, G., Djoko, D., Moennikes, O., Jeannet, C., Kondylis, A., Belushkin, M., 2017. Comparative assessment of HPHC yields in the tobacco heating system THS2.2 and commercial cigarettes. Regul. Toxicol. Pharmacol. 90, 1–8. https://doi.org/10.1016/j.yrtph.2017.08.006.

Jaunky, T., Adamson, J., Santopietro, S., Terry, A., Thorne, D., Breheny, D., Proctor, C., Gaça, M., 2018. Assessment of tobacco heating product THP1.0. Part 5: in vitro

dosimetric and cytotoxic assessment. Regul. Toxicol. Pharmacol. 93, 52–61. https://doi.org/10.1016/j.yrtph.2017.09.016.
Jones, J., Slayford, S., Gray, A., Brick, K., Prasad, K., Proctor, C., 2020. A cross-category puffing topography, mouth level exposure and consumption study among Italian users of tobacco and nicotine products. Sci. Rep. 10 (1), 12. https://doi.org/10.1038/s41598-019-55410-5.
Kogel, U., Gonzalez Suarez, I., Xiang, Y., Dossin, E., Guy, P., Mathis, C., Marescotti, D., Goedertier, D., Martin, F., Peitsch, M., Hoeng, J., 2015. Biological impact of cigarette smoke compared to an aerosol produced from a prototypic modified risk tobacco product on normal human bronchial epithelial cells. Toxicol. in Vitro 29 (8), 2102–2115. https://doi.org/10.1016/j.tiv.2015.08.004.
Leigh, N., Tran, P., O'Connor, R., Goniewicz, M., 2018. Cytotoxic effects of heated tobacco products (HTP) on human bronchial epithelial cells. Tob. Control. 27 (Suppl. 1), s26 https://doi.org/10.1136/tobaccocontrol-2018-054317.
Li, Y., Cui, H., Chen, L., Fan, M., Cai, J., Guo, J., Yurteri, C., Si, X., Liu, S., Xie, F., Xie, J., 2021. Modeled respiratory tract deposition of smoke aerosol from conventional cigarettes, electronic cigarettes and heat-not-burn products. Aerosol Air Qual. Res. 21 (5), 200241 https://doi.org/10.4209/aaqr.200241.
Liu, T, Zhang, L, Joo, D, Sun, SC, 2017. NF-κB signaling in inflammation. Signal Transduct Target. Ther 2, 17023. https://doi.org/10.1038/sigtrans.2017.23. Epub 2017 Jul 14. PMID: 29158945; PMCID: PMC5661633.
Lüdicke, F., Baker, G., Magnette, J., Picavet, P., Weitkunat, R., 2017. Reduced exposure to harmful and potentially harmful smoke constituents with the tobacco heating system 2.1. Nicotine Tob. Res. 19 (2), 168–175. https://doi.org/10.1093/ntr/ntw164.
Mallock, N., Böss, L., Burk, R., Danziger, M., Welsch, T., Hahn, H., 2018. Levels of selected analytes in the emissions of "heat not burn" tobacco products that are relevant to assess human health risks. Arch. Toxicol. 92 (6), 2145–2149.
McNeill, A., Munafò, M.R., 2013. Reducing harm from tobacco use. J. Psychopharmacol. 27, 13–18. https://doi.org/10.1177/0269881112458731.
McNeill, A., Brose, L., Calder, R., Bauld, L., Robson, D., 2018. Evidence Review of E-Cigarettes and Heated Tobacco Products 2018. A Report Commissioned by Public Health England. Public Health England, London.
McQuillan, K., Carr, T., Taylor, M., Bishop, E., Fearon, I., 2015. Examination of the use of human sera as an exposure agent for in vitro studies investigating the effects of cigarette smoking on cellular cardiovascular disease models. Toxicol. in Vitro 29 (5), 856–863. https://doi.org/10.1016/j.tiv.2015.03.008.
Motoyama, S., Takeiri, A., Tanaka, K., Harada, A., Matsuzaki, K., Taketo, J., Matsuo, S., Fujii, E., Mishima, M., 2018. Advantages of evaluating γH2AX induction in non-clinical drug development. Genes Environ. 40 (1), 10. https://doi.org/10.1186/s41021-018-0098-z.
Murphy, J., Liu, C., McAdam, K., Gaça, M., Prasad, K., Camacho, O., McAughey, J., Proctor, C., 2018. Assessment of tobacco heating product THP1.0. Part 9: the placement of a range of next-generation products on an emissions continuum relative to cigarettes via pre-clinical assessment studies. Regul. Toxicol. Pharmacol. 93, 92–104. https://doi.org/10.1016/j.yrtph.2017.10.001.
Nur-E-Kamal, A., Gross, S., Pan, Z., Balklava, Z., Ma, J., Liu, L., 2004. Nuclear translocation of cytochrome c during apoptosis. J. Biol. Chem. 279 (24), 24911–24914. https://doi.org/10.1074/jbc.C400051200.
OECD, 2016. Test No. 487: In Vitro Mammalian Cell Micronucleus Test, OECD Guidelines for the Testing of Chemicals, Section 4. OECD Publishing, Paris. https://doi.org/10.1787/9789264264861-en.
OECD, 2020. Test No. 471: Bacterial Reverse Mutation Test, OECD Guidelines for the Testing of Chemicals, Section 4. OECD Publishing, Paris. https://doi.org/10.1787/9789264071247-en.
Ogden, M., Marano, K., Jones, B., Morgan, W., Stiles, M., 2015. Switching from usual brand cigarettes to a tobacco-heating cigarette or snus: part 2. Biomarkers of exposure. Biomarkers 20 (6–7), 391–403. https://doi.org/10.3109/1354750X.2015.1094134.
O'Leary, R., Polosa, R., 2020. Tobacco harm reduction in the 21st century. Drugs Alcohol Today 20 (3), 219–234. https://doi.org/10.1108/dat-02-2020-0007.
Perezhogina, T., Gnuchhikh, E., Faizullin, R., Medvedeva, S., Zaytseva, T., Duruncha, A., et al., 2021. Investigation of volatile organic compounds and benzo[a]pyrene contents in the aerosols of cigarettes and IQOS tobacco heating system using high-performance gas chromatography/mass spectrometry. BioNanoScience. https://doi.org/10.1007/s12668-021-00898-3.
Phillips-Waller, A., Przulj, D., Pesola, F., Smith, K., Hajek, P., 2021. Nicotine delivery and user ratings of IQOS heated tobacco system compared with cigarettes, juul, and refillable E-cigarettes. Nicotine Tob. Res. 23 (11), 1889–1894.
Picavet, P., Haziza, C., Lama, N., Weitkunat, R., Lüdicke, F., 2016. Comparison of the pharmacokinetics of nicotine following single and ad libitum use of a tobacco heating system or combustible cigarettes. Nicotine Tob. Res. 18 (5), 557–563. https://doi.org/10.1093/ntr/ntv220.
Poussin, C., Laurent, A., Peitsch, M., Hoeng, J., De Leon, H., 2016. Systems toxicology-based assessment of the candidate modified risk tobacco product THS2.2 for the adhesion of monocytic cells to human coronary arterial endothelial cells. Toxicology 339, 73–86. https://doi.org/10.1016/j.tox.2015.11.007.
Poussin, C., Laurent, A., Kondylis, A., Marescotti, D., van der Toorn, M., Guedj, E., Goedertier, D., Acali, S., Pak, C., Dulize, R., Baumer, K., Peric, D., Maluenda, E., Bornand, D., Gonzalez Suarez, I., Schlage, W., Ivanov, N., Peitsch, M., Hoeng, J., 2018. In vitro systems toxicology-based assessment of the potential modified risk tobacco product CHTP 1.2 for vascular inflammation- and cytotoxicity-associated mechanisms promoting adhesion of monocytic cells to human coronary arterial endothelial cells. Food Chem. Toxicol. 120, 390–406. https://doi.org/10.1016/j.fct.2018.07.025.
Reif, D., Sypa, M., Lock, E., Wright, F., Wilson, A., Cathey, T., Judson, R., Rusyn, I., 2013. ToxPi GUI: an interactive visualization tool for transparent integration of data from diverse sources of evidence. Bioinformatics 29 (3), 402–403. https://doi.org/10.1093/bioinformatics/bts686.
Roulet, S., Mainy, N., Chrea, C., Magnani, P., Weitkunat, R., Kallischnigg, G., Ramazzotti, A., 2017. Pre-market studies from five countries in Asia and Europe to measure the adoption of the tobacco heating system (THS) in smokers. Tob. Sci. Technol. 50 (13), 86. https://doi.org/10.16135/j.issn1002-0861.2017.0564.
Roulet, S., Chrea, C., Kanitscheider, C., Kallischnigg, G., Magnani, P., Weitkunat, R., 2019. Potential predictors of adoption of the tobacco heating system by U.S. adult smokers: an actual use study. F1000Res 8, 214. https://doi.org/10.12688/f1000research.17606.1.
Royal College of Physicians, 2016. Nicotine Without Smoke: Tobacco Harm Reduction. https://www.rcplondon.ac.uk/projects/outputs/nicotine-without-smoke-tobacco-harm-reduction-0 (Accessed 14-02-2021).
Rudd, K., Stevenson, M., Wieczorek, R., Pani, J., Trelles Sticken, E., Dethloff, O., Czekala, L., Simms, L., Buchanan, F., O'Connell, G., Walele, T., 2020. Chemical composition and in vitro toxicity profile of a pod-based E-cigarette aerosol compared to cigarette smoke. App. Vitro Toxicol. 6 (1), 11–41. https://doi.org/10.1089/aivt.2019.0015.
Sakaguchi, C., Kakehi, A., Minami, N., Kikuchi, A., Futamura, Y., 2014. Exposure evaluation of adult male Japanese smokers switched to a heated cigarette in a controlled clinical setting. Regul. Toxicol. Pharmacol. 69 (3), 338–347. https://doi.org/10.1016/j.yrtph.2014.04.016.
Schaller, J.-P., Keller, D., Poget, L., Pratte, P., Kaelin, E., McHugh, D., Cudazzo, G., Smart, D., Tricker, A., Gautier, L., Yerly, M., Reis Pires, R., Le Bouhellec, S., Ghosh, D., Hofer, I., Garcia, E., Vanscheeuwijck, P., Maeder, S., 2016. Evaluation of the tobacco heating system 2.2. Part 2: chemical composition, genotoxicity, cytotoxicity, and physical properties of the aerosol. Regul. Toxicol. Pharmacol. 81, S27–S47. https://doi.org/10.1016/j.yrtph.2016.10.001.
Scharf, P., da Rocha, G., Sandri, S., Heluany, C., Pedreira Filho, W., Farsky, S., 2021. Immunotoxic mechanisms of cigarette smoke and heat-not-burn tobacco vapor on Jurkat T cell functions. Environ. Pollut. 268, 115863 https://doi.org/10.1016/j.envpol.2020.115863.
Simms, L., Rudd, K., Palmer, J., Czekala, L., Yu, F., Chapman, F. Trelles, Sticken, E., Wieczorek, R., Bode, L., Stevenson, M., Walele, T., 2020. The use of human induced pluripotent stem cells to screen for developmental toxicity potential indicates reduced potential for non-combusted products, when compared to cigarettes. Curr. Res. Toxicol. 1, 161–173. https://doi.org/10.1016/j.crtox.2020.11.001.
Smart, D.J., Phillips, G., 2021. Collecting e-cigarette aerosols for in vitro applications: a survey of the biomedical literature and opportunities to increase the value of submerged cell culture-based assessments. J. Appl. Toxicol. 41 (1), 161–174. https://doi.org/10.1002/jat.4064.
Smith, M., Clark, B., Lüdicke, F., Schaller, J.-P., Vanscheeuwijck, P., Hoeng, J., Peitsch, M., 2016. Evaluation of the tobacco heating system 2.2. Part 1: description of the system and the scientific assessment program. Regul. Toxicol. Pharmacol. 81, S17–S26. https://doi.org/10.1016/j.yrtph.2016.07.006.
Solier, S., Pommier, Y., 2009. The apoptotic ring: a novel entity with phosphorylated histones H2AX and H2B and activated DNA damage response kinases. Cell Cycle 8, 1853–1859. https://doi.org/10.4161/cc.8.12.8865.
Taylor, M., Jaunky, T., Hewitt, K., Breheny, D., Lowe, F., Fearon, I., Gaca, M., 2017. A comparative assessment of e-cigarette aerosols and cigarette smoke on in vitro endothelial cell migration. Toxicol. Lett. 277, 123–128. https://doi.org/10.1016/j.toxlet.2017.06.001.
Taylor, M., Thorne, D., Carr, T., Breheny, D., Walker, P., Proctor, C., Gaça, M., 2018. Assessment of novel tobacco heating product THP1.0. Part 6: a comparative in vitro study using contemporary screening approaches. Regul. Toxicol. Pharmacol. 93, 62–70. https://doi.org/10.1016/j.yrtph.2017.08.016.
Thorne, D., Breheny, D., Proctor, C., Gaca, M., 2018. Assessment of novel tobacco heating product THP1.0. Part 7: comparative in vitro toxicological evaluation. Regul. Toxicol. Pharmacol. 93, 71–83. https://doi.org/10.1016/j.yrtph.2017.08.017.
Thorne, D., Leverette, R., Breheny, D., Lloyd, M., McEnaney, S., Whitwell, J., Clements, J., Bombick, B., Gaça, M., 2019. Genotoxicity evaluation of tobacco and nicotine delivery products: part two. In vitro micronucleus assay. Food Chem. Toxicol. 132, 110546. https://doi.org/10.1016/j.fct.2019.05.054.
Thorne, D., Whitwell, J., Clements, J., Walker, P., Breheny, D., Gaca, M., 2020. The genotoxicological assessment of a tobacco heating product relative to cigarette smoke using the in vitro micronucleus assay. Toxicol. Rep. 7, 1010–1019. https://doi.org/10.1016/j.toxrep.2020.08.013.
Trask Jr., O.J., 2012. Nuclear factor Kappa B (NF-κB) translocation assay development and validation for high content screening. In: Markossian, S., Sittampalam, G.S., Grossman, A., et al. (Eds.), Assay Guidance Manual [Internet]. Bethesda (MD): Eli Lilly & Company and the National Center for Advancing Translational Sciences; 2004. Available from: https://www.ncbi.nlm.nih.gov/books/NBK100914/ (Accessed 15-02-2021).
Trombetta, D., Castelli, F., Grazia Sarpietro, M., Venuti, V., Cristani, M., Daniele, C., Saija, A., Mazzanti, G., Bisignano, G., 2005. Mechanisms of antibacterial action of three monoterpenes. Antimicrob. Agents Chemother. 49 (6), 2474–2478. https://doi.org/10.1128/AAC.49.6.2474-2478.2005.
United States Surgeon General, 2010. Surgeon General's Report – How Tobacco Smoke Causes Disease: The Biology and Behavioural Analysis for Smoking-Attributable Disease. https://www.cdc.gov/tobacco/data_statistics/sgr/2010/index.htm.
US Department of Health and Human Services, 2014. The health consequences of smoking–50 years of progress: a report of the surgeon general. Atlanta, GA. In: US Department of Health and Human Services, Centers for Disease Control and

Prevention, National Center for Chronic Disease Prevention and Health Promotion, Office on Smoking and Health.

van der Toorn, M., Frentzel, S., De Leon, H., Goedertier, D., Peitsch, M., Hoeng, J., 2015. Aerosol from a candidate modified risk tobacco product has reduced effects on chemotaxis and transendothelial migration compared to combustion of conventional cigarettes. Food Chem. Toxicol. 86, 81–87. https://doi.org/10.1016/j.fct.2015.09.016.

Wang, H., Chen, H., Huang, L., Li, X., Wang, L., Li, S., Liu, M., Zhang, M., Han, S.J.X., Fu, Y., Tian, Y., Hou, H., Hu, Q., 2021. In vitro toxicological evaluation of a tobacco heating product THP COO and 3R4F research reference cigarette on human lung cancer cells. Toxicol. in Vitro 74, 105173. https://doi.org/10.1016/j.tiv.2021.105173.

Wieczorek, R., Phillips, G., Czekala, L., Trelles Sticken, E., O'Connell, G., Simms, L., Rudd, K., Stevenson, M., Walele, T., 2020. A comparative in vitro toxicity assessment of electronic vaping product e-liquids and aerosols with tobacco cigarette smoke. Toxicol. in Vitro 66, 104866. https://doi.org/10.1016/j.tiv.2020.104866.

Wilde, E., Chapman, K., Stannard, L., Seager, A., Brüsehafer, K., Shah, U., Tonkin, J., Brown, R., Verma, J., Doherty, A., Johnson, G., Doak, S., Jenkins, G., 2018. A novel, integrated in vitro carcinogenicity test to identify genotoxic and non-genotoxic carcinogens using human lymphoblastoid cells. Arch. Toxicol. 92 (2), 935–951. https://doi.org/10.1007/s00204-017-2102-y.

Williams, R., DeMarini, D., Stankowski Jr., L., Escobard, P., Zeiger, E., Howe, J., Elespurug, R., Crossh, K., 2019. Are all bacterial strains required by OECD mutagenicity test guideline TG471 needed? Mutat. Res. Genet. Toxicol. Environ. Mutagen. 848, 503081 https://doi.org/10.1016/j.mrgentox.2019.503081.

Zeller, M., 2019. The future of nicotine regulation: key questions and challenges. Nicotine Tob. Res. 21 (3), 331–332. https://pubmed.ncbi.nlm.nih.gov/23035032/.